

AD-767 559

INVESTIGATION OF THE MANEUVERABILITY OF  
THE S-67 WINGED HELICOPTER

Robert A. Monteleone

United Aircraft Corporation

Prepared for:

Army Air Mobility Research and Development  
Laboratory

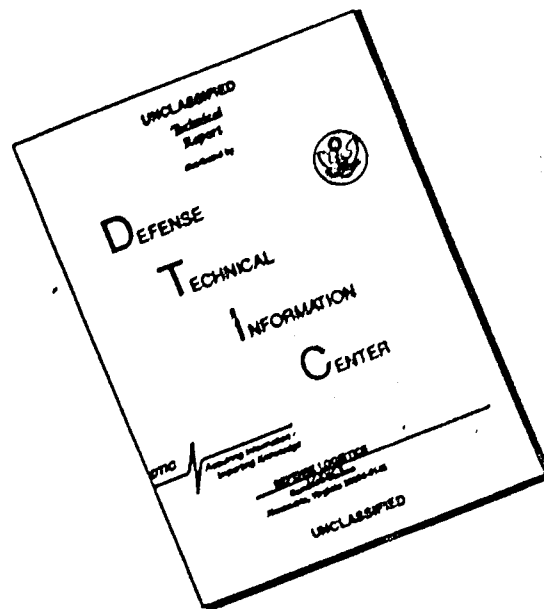
June 1973

DISTRIBUTED BY:

**NTIS**

National Technical Information Service  
U. S. DEPARTMENT OF COMMERCE  
5285 Port Royal Road, Springfield Va. 22151

# DISCLAIMER NOTICE



THIS DOCUMENT IS BEST QUALITY AVAILABLE. THE COPY FURNISHED TO DTIC CONTAINED A SIGNIFICANT NUMBER OF PAGES WHICH DO NOT REPRODUCE LEGIBLY.

AD

## USAAMRDL TECHNICAL REPORT 73-51

# INVESTIGATION OF THE MANEUVERABILITY OF THE S-67 WINGED HELICOPTER

By

Robert A. Monteleone

June 1973

EUSTIS DIRECTORATE  
U. S. ARMY AIR MOBILITY RESEARCH AND DEVELOPMENT LABORATORY  
FORT EUSTIS, VIRGINIA

CONTRACT DAAJ02-71-C-0008  
UNITED AIRCRAFT CORPORATION  
SIKORSKY AIRCRAFT DIVISION  
STRATFORD, CONNECTICUT

Approved for public release;  
distribution unlimited.



Reproduced by  
NATIONAL TECHNICAL  
INFORMATION SERVICE  
U.S. Department of Commerce  
Springfield, VA 22151

AD 767559

#### DISCLAIMERS

The findings in this report are not to be construed as an official Department of the Army position unless so designated by other authorized documents.

When Government drawings, specifications, or other data are used for any purpose other than in connection with a definitely related Government procurement operation, the United States Government thereby incurs no responsibility nor any obligation whatsoever; and the fact that the Government may have formulated, furnished, or in any way supplied the said drawings, specifications, or other data is not to be regarded by implication or otherwise as in any manner licensing the holder or any other person or corporation, or conveying any rights or permission, to manufacture, use, or sell any patented invention that may in any way be related thereto.

Trade names cited in this report do not constitute an official endorsement or approval of the use of such commercial hardware or software.

#### DISPOSITION INSTRUCTIONS

Destroy this report when no longer needed. Do not return it to the originator.

A

;

UNCLASSIFIED

Security Classification

## DOCUMENT CONTROL DATA - R &amp; D

(Security classification of title, body of abstract and indexing annotation must be entered when the overall report is classified)

1. ORIGINATING ACTIVITY (Corporate author) UNITED AIRCRAFT CORPORATION SIKORSKY AIRCRAFT DIVISION STRATFORD, CONNECTICUT		2a. REPORT SECURITY CLASSIFICATION UNCLASSIFIED	
		2b. GROUP	
3. REPORT TITLE INVESTIGATION OF THE MANEUVERABILITY OF THE S-67 WINGED HELICOPTER			
4. DESCRIPTIVE NOTES (Type of report and inclusive dates) Final Report			
5. AUTHOR(S) (First name, middle initial, last name) Robert A. Monteleone			
6. REPORT DATE June 1973		7a. TOTAL NO. OF PAGES 69 71	7b. NO. OF REFS 9
8a. CONTRACT OR GRANT NO. DAAJ02-71-C-0008		9a. ORIGINATOR'S REPORT NUMBER(S) USAAMRDL Technical Report 73-51	
b. PROJECT NO.		9b. OTHER REPORT NO(S) (Any other numbers that may be assigned this report)	
c. Task 1F163204D15704			
d.			
10. DISTRIBUTION STATEMENT  Approved for public release; distribution unlimited.			
11. SUPPLEMENTARY NOTES		12. SPONSORING MILITARY ACTIVITY EUSTIS DIRECTORATE U.S. ARMY AIR MOBILITY R&D LABORATORY FORT EUSTIS, VIRGINIA	
13. ABSTRACT  A flight test program and a computer simulation study have been conducted to evaluate the maneuverability and speed capability of the S-67 as a representative winged helicopter design. The flight program evaluated the effects on load factor capability of wings and of variations in gross weight, center of gravity, stabilator bias angle, and type of maneuver. The computer simulation determined the effects of stabilator linkage changes, of several control system feedbacks, and of differential speed brake application for roll control.  Program results show that helicopter maneuverability can be improved by the addition of wings. Main rotor control system loads were the limiting factor on maneuver capability of the S-67. Control load buildup is minimized when rotor torque is low.  Wings increased speed capability somewhat by delaying rotor stall effects. The dynamic stability of the S-67 satisfies MIL-H-8501A requirements above 100 knots.			

DD FORM 1473

REPLACES DD FORM 1473, 1 JAN 64, WHICH IS OBSOLETE FOR ARMY USE.

UNCLASSIFIED

Security Classification

1a

UNCLASSIFIED

Security Classification

14 KEY WORDS	LINK A		LINK B		LINK C	
	ROLE	WT	ROLE	WT	ROLE	WT
Aerodynamics						
Blackhawk Maneuverability						
Constant Airspeed Turns						
Controllability						
Control Loads						
Descending Turns						
Diving Pull-ups						
Dynamic Stability						
Envelope of Airspeed and Load Factor						
Flight Test						
"G" Capability						
Gross-Weight Effect on Rotor Lift						
Helicopter						
Integrated Controls						
Lift Sharing						
Load Factor						
Maneuverability						
Normal Load Factor						
Operational Maneuver Capability						
Performance of Winged Helicopters						
Pitch-Rate Effect on Rotor Stall						
Roll Reversals						
Rotary Wing						
Sikorsky S-67						
Simulation						
Speed Brakes						
Speed Capability						
Spoilers						
Stabilator Bias Angle						
Stability and Control						
Steady Turns						
Torque Effect on Rotor Lift						
Unloading Rotors						
Vibratory Control Loads						
VTOL Flight						
Winged Helicopter						
Yawing Stability						

UNCLASSIFIED

Security Classification



DEPARTMENT OF THE ARMY  
U. S. ARMY AIR MOBILITY RESEARCH & DEVELOPMENT LABORATORY  
EUSTIS DIRECTORATE  
FORT EUSTIS, VIRGINIA 23604

This report was prepared by United Aircraft Corporation, Sikorsky Aircraft Division, under Contract DAAJ02-71-C-0008.

This program was a flight investigation of the maneuverability and speed capability of the S-67 as a representative winged helicopter design. A computer simulation was included to determine the effects of stabilator linkage changes, several control system feedbacks, and differential speed brake application for roll control.

The addition of wings to the S-67 improves the maneuvering load factor capability to a significant degree. Control coupling variations have little effect on load sharing. Main rotor control system loads are the limiting factor in determination of the maneuver capability of the S-67. Control load buildup is minimized when rotor torque is low. Roll capability is slightly reduced by the S-67 wing configuration; however, analysis shows that the use of differential speed brakes can more than compensate for this change. Wings improve level-flight speed capability by delaying drag rise and control load buildup due to rotor stall.

The report has been reviewed by this Directorate and is technically correct.

This program was conducted under the technical management of Mr. R. C. Dumond of the Systems Support Division.

Task 1F163204D15704  
Contract DAAJ02-71-C-0008  
USAAMRDL Technical Report 73-51  
June 1973

INVESTIGATION OF THE MANEUVERABILITY  
OF THE S-67 WINGED HELICOPTER

SER-67008

By

Robert A Monteleone

Prepared by

United Aircraft Corporation  
Sikorsky Aircraft Division  
Stratford, Connecticut

for

EUSTIS DIRECTORATE  
U. S. ARMY AIR MOBILITY RESEARCH AND DEVELOPMENT LABORATORY  
FORT EUSTIS, VIRGINIA

Approved for public release; distribution unlimited.

### ABSTRACT

A flight test program and a computer simulation study have been conducted to evaluate the maneuverability and speed capability of the S-67 as a representative winged helicopter design. The flight program evaluated the effects on load factor capability of wings and of variations in gross weight, center of gravity, stabilator bias angle, and type of maneuver. The computer simulation determined the effects of stabilator linkage changes, of several control system feedbacks, and of differential speed brake application for roll control.

Program results show that helicopter maneuverability can be improved by the addition of wings. Main rotor control system loads were the limiting factor on maneuver capability of the S-67. Control load buildup is minimized when rotor torque is low.

Wings increased speed capability somewhat by delaying rotor stall effects. The dynamic stability of the S-67 satisfies MIL-H-8501A requirements above 100 knots.

## FOREWORD

This report presents results of flight tests and computer simulations to evaluate the maneuverability and speed capability of the Sikorsky S-67 aircraft. This program is part of a four-phase investigation of the flight characteristics of the S-67 aircraft as a representative high-speed winged helicopter. Investigations of the stabilator, speed brakes, and a longitudinal stick feel augmentation system are also part of the flight investigation of the S-67.

The work was performed by the Sikorsky Aircraft Division of United Aircraft Corporation for the Eustis Directorate, U.S. Army Air Mobility Research and Development Laboratory, Fort Eustis, Virginia, under Contract DAAJ02-71-C-0008, DA Task 1F163204D15704. Mr. R. C. Dumond was the Army Technical Representative.

## TABLE OF CONTENTS

	<u>Page</u>
ABSTRACT. . . . .	iii
FOREWORD. . . . .	v
LIST OF ILLUSTRATIONS . . . . .	viii
LIST OF SYMBOLS . . . . .	xi
INTRODUCTION. . . . .	1
SCOPE OF PROGRAM. . . . .	2
DESCRIPTION OF AIRCRAFT AND SIMULATION. . . . .	5
TEST PROCEDURES . . . . .	8
RESULTS AND DISCUSSION. . . . .	9
LOAD FACTOR CAPABILITY. . . . .	9
Results . . . . .	9
Effect of Rotor Torque. . . . .	9
Effect of Gross Weight. . . . .	10
Effect of Wings . . . . .	10
AIRCRAFT STABILITY. . . . .	13
Longitudinal Dynamic Stability. . . . .	13
Lateral-Directional Stability . . . . .	13
SIMULATION STUDIES. . . . .	14
CONCLUSIONS . . . . .	15
LITERATURE CITED. . . . .	16
DISTRIBUTION. . . . .	58

# LIST OF ILLUSTRATIONS

<u>Figure</u>		<u>Page</u>
1	S-67 Three-View Drawing . . . . .	17
2	S-67 in Flight, Front View. . . . .	18
3	S-67 Main Rotor Pylon With Prototype Flow Separator . . . . .	19
4	S-67 Quarter View Without Wings . . . . .	20
5	S-67 Gross-Weight and Center-of-Gravity Envelope. . . . .	21
6	S-67 Wind Tunnel Data Showing the Effect of Wings on Lift, Drag, and Pitching Moment Parameters. . . . .	22
7	S-67 Wind Tunnel Data Showing the Effect of the Vertical Tail on Side Force, Yawing Moment, and Rolling Moment Parameters. . . . .	23
8	S-67 Wind Tunnel Data Showing the Effect of Various Speed Brake Combinations on Rolling Moment. . . . .	24
9	S-67 Longitudinal Cyclic, Rate of Descent, Control Load, Collective, and Engine Torque vs Load Factor at 14,800 Lb, 276 C.G. in Steady Turns . . . . .	25
10	S-67 Summary of Load Factor Data vs Airspeed at 14,800 Lb, 276 C.G., Showing the Effects of Maneuver Condition and Stabilator Bias Angle . . . . .	28
11	S-67 Symmetrical Pull-Up at 180 KCAS, 14,800 Lb, 276 C.G., 2.5 Deg Stabilator Bias Angle . . . . .	29
12	S-67 Longitudinal Cyclic, Control Load, Collective, and Engine Torque vs Load Factor at 14,800 Lb, 276 C.G. in Symmetrical Pull-Ups. . . . .	30
13	S-67 Longitudinal Cyclic, Rate of Descent, Control Load, Collective, and Engine Torque vs Load Factor at 17,300 Lb, 276 C.G., 180 KCAS in Steady Turns. . . . .	33
14	S-67 Summary of Load Factor Data vs Airspeed at 17,300 Lb, Showing the Effects of Maneuver Condition, Stabilator Bias Angle, and C.G. . . . .	34
15	S-67 Comparison of Level-Flight Data at Forward and Aft C.G. at 17,300 Lb, 2.5 Deg Stabilator Bias Angle. . . . .	36

<u>Figure</u>		<u>Page</u>
16	S-67 Summary of Load Factor Data vs Airspeed at 14,800 Lb, 276 C.G., Without Wings, Showing the Effects of Maneuver Condition, Wings, and Stabilator Bias Angle. . . . .	37
17	S-67 Comparison of Level-Flight Data With and Without Wings at 14,800 Lb, 276 C.G. . . . .	38
18	S-67 Load Factor vs Airspeed at 14,800 Lb, 276 C.G., Constant Engine Torque, Comparing Steady Turns and Pull-Ups . . . . .	39
19	S-67 Summary of Engine Torque vs Load Factor at 14,800 Lb, 276 C.G., Without Wings, for Various Speeds and Maneuvers. . .	40
20	S-67 Load Factor Capability vs Airspeed at Constant Engine Torques and Gross Weights, Derived From Control-Load-Limited Flight Data at 3000 Ft Density Altitude. . . . .	41
21	S-67 Longitudinal Stability, AFCS Off, at 14,800 Lb, 276 C.G., 140 KCAS, Following an Aft Cyclic Pulse. . . . .	42
22	S-67 Summary of Longitudinal Characteristic Roots Derived From Time Histories of Aircraft Motion Following Control Pulses, AFCS Off, 14,800 Lb, 276 C.G.. . . . .	43
23	S-67 Lateral-Directional Trim Characteristics, Showing the Effect of Wings at 14,800 Lb, 276 C.G. . . . .	44
24	S-67 Lateral-Directional Stability, AFCS Off, at 14,800 Lb, 276 C.G., 140 KCAS, Following a Left Lateral Cyclic Pulse. . . . .	45
25	S-67 Lateral-Directional Stability, AFCS Off, at 14,800 Lb, 276 C.G., 140 KCAS, Following a Right Pedal Pulse. . . . .	46
26	S-67 Summary of Lateral and Directional Characteristic Roots Derived From Time Histories of Aircraft Motion Following Control Pulses, AFCS Off, 14,800 Lb, 276 C.G.. . . .	47
27	S-67 Roll Reversal at 180 KCAS, 14,800 Lb, 276 C.G., 2.5 Deg Stabilator Bias Angle. . . . .	48
28	S-67 Roll Reversal at 170 KCAS, Without Wings, 14,800 Lb, 276 C.G., 4.5 Deg Stabilator Bias Angle. . . . .	49
29	S-67 Roll Rate vs Lateral Cyclic, Showing the Effect of Wings at 14,800 Lb, 276 C.G. . . . .	50

FigurePage

30	S-67 Simulator Data - Effect of Stick to Stabilator Gain in 180-KCAS, 2800-HP, Steady-State Descending Turns at 14,800 Lb, 276 C.G. . . . .	51
31	S-67 Simulator Data - Effect of Stabilator Bias Angle in 180-KCAS, 2800-HP, Steady-State Descending Turns at 14,800 Lb, 276 C.G. . . . .	52
32	S-67 Simulator Data - Effect of Pitch Rate Feedback to Rotor Cyclic in 180-KCAS, 2800-HP, Steady-State Descending Turns at 14,800 Lb, 276 C.G. . . . .	53
33	S-67 Simulator Data - Effect of Load Factor Feedback to Rotor Cyclic in 180-KCAS, 2800-HP, Steady-State Descending Turns at 14,800 Lb, 276 C.G. . . . .	54
34	S-67 Simulator Data - Effect of Load Factor Coupling to Stabilator Incidence in 180-KCAS, 2800-HP, Steady-State Descending Turns at 14,800 Lb, 276 C.G. . . . .	55
35	S-67 Simulator Data - Effect of Horsepower Variation in 180-KCAS, Steady-State Descending Turns at 14,800 Lb, 276 C.G. . . . .	56
36	S-67 Simulator Data - Roll Rate vs Lateral Cyclic, Showing the Effect of Integrated Spoilers at 14,800 Lb, 276 C.G. . . .	57

### LIST OF SYMBOLS

A	arbitrary constant of integration
$A_{1s}$	main rotor lateral cyclic pitch blade angle measured in shaft axis system, deg
AFCS	automatic flight control system
B	arbitrary constant of integration
$B_{1s}$	main rotor longitudinal cyclic pitch blade angle measured in shaft axis system, deg
b	wing span, ft
C	equivalent damping constant
C.G.	center of gravity, in.
$C_L$	lift coefficient, $1/2\rho V^2 S$
D	airframe drag, lb
G.W.	gross weight, lb
g	load factor
I	equivalent inertia constant
IFR	instrument flight rules
$I_t$	stabilator incidence, deg
$I_x$	rolling inertia, slug-ft <sup>2</sup>
$I_y$	pitching inertia, slug-ft <sup>2</sup>
$I_z$	yawing inertia, slug-ft <sup>2</sup>
$I_{xz}$	cross product of inertia, slug-ft <sup>2</sup>
J	mathematical symbol for imaginary numbers
K	equivalent spring constant
L	fuselage lift, lb
l	fuselage rolling moment, ft-lb
M	fuselage pitching moment, ft-lb

N	fuselage yawing moment, ft-lb
n	mathematical symbol for real numbers
p	fuselage roll angular velocity, rad/sec
Q	engine torque, %
q	dynamic pressure, lb/ft <sup>2</sup>
RLSS	right lateral stationary star, control load, lb
S	representative area, ft <sup>2</sup>
V	airspeed, KCAS
Y	fuselage side force, lb
$\alpha$	fuselage angle of attack, deg
$\beta$	fuselage sideslip angle, deg
$\lambda$	differential operator d/dt
$\rho$	air density, slugs/ft <sup>3</sup>
$\theta_0$	main rotor collective pitch blade angle measured at the center of rotation, deg
$\theta_f$	fuselage pitch attitude, deg
$\dot{\theta}_f$	fuselage pitch angular velocity, deg/sec
$\psi$	fuselage heading angle, deg
$\omega$	frequency of airframe oscillation, rad/sec

## INTRODUCTION

The lift capability of a helicopter rotor at high forward speeds is limited by retreating blade stall. This rotor blade stall may limit aircraft forward speed, and it usually restricts the maneuvering envelope at high speed. A fixed wing added to a helicopter can extend the lift capability, particularly at high speed, if the airloads can be distributed properly between rotor and wing.

Sikorsky has previously installed wings on the S-55 (H-19), the S-61R (CH-3C), and the S-61F (NH-3A) to determine the effect of wings on speed and maneuverability. In each case, speed improvements, if any, were small, but both the S-61R and S-61F showed maneuverability improvements. With this background, the S-67 wings were sized and incidence angle set such that at  $V_{max}$  in level flight, wing lift would be small. At lower speeds and higher angles of attack, the wing contribution to maneuverability would be significant, even though the dynamic pressure is lower.

The objective of this program was to evaluate the maneuverability and speed capability of the S-67 aircraft as a representative winged helicopter design. In addition, the computer simulation portion of the study was intended to correlate analytical methods with measured flight data, and to evaluate possible improvements in control coupling.

### SCOPE OF PROGRAM

A research flight test and computer simulation program investigated the effects of wings on the maneuverability characteristics of the Sikorsky S-67 helicopter. The flight test phase used three basic maneuvers for evaluation: (1) constant airspeed turns, (2) symmetrical diving pull-ups, and (3) roll reversals. Longitudinal and lateral-directional dynamic stability tests and lateral-directional static stability tests were also performed.

Listed below are the combinations of gross weight and center of gravity locations that were flown. A forward-C.G., light-gross-weight case was not flown, because it could be obtained only at a very low fuel load. The light-gross-weight, aft-C.G. case was reflown for evaluation with wings removed, since the maximum maneuver envelope was available for test at this weight.

<u>Loading Condition</u>	<u>Gross Weight (lb)</u>	<u>C.G. Location (in.)</u>
1	17,300	250
2	14,800	276
3	17,300	276

The stabilator bias angle and airspeed for each loading condition and maneuver investigated in the flight test program are listed in Table I.

An analytical evaluation was performed using a six-degree-of-freedom hybrid computer simulation. The simulation was correlated with the flight data, and then the effects of control system modifications were evaluated. Control modifications included: (1) stabilator trim bias angle changes, (2) stabilator/stick gain changes, (3) differential feedback between main rotor and stabilator control inputs, and (4) differential speed brake operation for roll control.

The analytical studies were performed at 14,800 lb, 276 in. C.G. Table II lists the simulated control system modifications evaluated in 180-KCAS turns. Roll rate calculations with differential speed brakes were made at 140 and 180 KCAS.

TABLE I. FLIGHT TEST CONDITIONS

Flight Condition	Airspeed (KCAS)	Wings	Stabilator Bias Angle (deg)		
			Loading Condition 1	Loading Condition 2	Loading Condition 3
Constant-Airspeed Turns	100,140,180	on off	0.5,2.5,4.5 -	0.5,2.5,4.5 2.5,4.5	0.5,2.5,4.5 -
Symmetrical Diving Pull-Ups	140,180,200	on off	0.5,2.5,4.5 -	0.5,2.5,4.5 4.5	0.5,2.5,4.5 -
Roll Reversals	100,140,180	on off	- -	2.5 4.5	- -
Lateral-Directional Static Stability	100,140,180	on off	- -	2.5 4.5	- -
Dynamic Stability	100,140,180	on	-	2.5	-

TABLE II. SIMULATED LONGITUDINAL CONTROL SYSTEM VARIATIONS

Case	Figure	Stabilator Blow Angle (deg)	Coupling Gains*			
			$I_t/B_{1_s}$	$B_{1_s}/\dot{\theta}_f$	$B_{1_s}/g$	$I_t/g$
1	28	2.5	0.5	0	0	0
2	28	2.5	1.0	0	0	0
3	28	2.5	2.0	0	0	0
4	29	0	1.0	0	0	0
5	29	5.0	1.0	0	0	0
6	30	2.5	1.0	0.2	0	0
7	30	2.5	1.0	0.5	0	0
8	31	2.5	1.0	0	2.0	0
9	31	2.5	1.0	0	4.0	0
10	32	2.5	1.0	0	0	-2.5
11	32	2.5	1.0	0	0	-5.0

\* Modified Control Coupling      \*\* Basic S-67 Configuration

Delta Rotor Cyclic =  $(B_{1_s}/\dot{\theta}_f)$  (Pitch Rate) +  $(B_{1_s}/g)$  (Load Factor)Delta Stabilator Incidence =  $(I_t/B_{1_s})$  (Rotor Cyclic) +  $(I_t/g)$  (Load Factor)

## DESCRIPTION OF AIRCRAFT AND SIMULATION

The S-67 demonstrator aircraft is a high-speed derivative of the Sikorsky S-61 (SH-3D) helicopter. The narrow, low-drag airframe was designed for high speed. The cockpit is arranged in tandem, with the copilot-runner in the forward seat and the pilot in the elevated aft seat. The pilot has visibility down to minus 15 degrees over the nose. Two T58-GE-5 engines are mounted in the main rotor pylon above the fuselage center section.

The main rotor hub, tail rotor, drive system, and transmission system are all SH-3D dynamic components. The main rotor has five S-61F blades, each with a twist of -4 degrees. The 22-inch blade tips are swept back 20 degrees, thinned, and cambered to delay tip Mach number effects. The rotor control system uses SH-3D components.

The fixed-wing type surfaces include the stabilator, a vertical stabilizer, and sponsons with stub wings. The vertical stabilizer is fixed. The tail wheel is attached to the base of the ventral fin, and the retractable main landing gear is housed in the wing sponsons. Wings are attached to the sponsons for additional lift, and attachment points for armament are provided. The wing panels have speed brakes to control dive angle and increase deceleration capability.

A three-view drawing of the S-67 is provided in Figure 1. Prior to the maneuver flight tests, the tail rotor diameter was changed from 10 ft 4 in. to 10 ft 7 in., and a main rotor pylon flow separator was added to reduce tail-shake vibrations. Figures 2 through 4 are photographs of the test aircraft. Figure 5 shows the weight and center-of-gravity envelope for the demonstrator aircraft, including the flight-test points.

Principal dimensions and general data for the S-67 aircraft are as follows:

### Main Rotor

Diameter	62 ft
Normal Tip Speed (104 percent $N_R$ )	686 ft/sec
Disc Area	3019 ft <sup>2</sup>
Solidity	0.0781
Number of Blades	5
Blade Chord	1.52 ft
Blade Twist	-4 deg
Airfoil Section	NACA 0012 MOD
Articulation	Full flapping and lagging
Tip Sweep	20 deg

### Tail Rotor

Diameter	10 ft 7 in.
Tip Speed	718 ft/sec
Disc Area	87.9 ft <sup>2</sup>
Solidity	0.1843
Number of Blades	5

### Tail Rotor (cont'd)

Blade Chord	0.612 ft
Blade Twist	0 deg
Airfoil Section	NACA 0012 MOD
Pitch Flap Coupling	45 deg

### Fuselage

Overall Length	64 ft 1 in.
Overall Height	16 ft 3 in.
Overall Width	27 ft 4 in.
Wheel Tread	7 ft
Wheel Base	36 ft 2 in.

### Stabilator

Root Chord	4 ft 2 in.
Tip Chord	2 ft
Taper Ratio	0.48
Area	50 ft <sup>2</sup>
Span	15 ft 6 in.
Aspect Ratio	4.8
Airfoil (Root)	NACA 0015
Airfoil (Tip)	NACA 0012

### Vertical Fin

Root Chord	7 ft 6 in.
Tip Chord (Upper)	2 ft 10 in.
Tip Chord (Lower)	3 ft 9 in.
Taper Ratio (Upper)	0.62
Taper Ratio (Lower)	0.5
Total Area	68.7 ft <sup>2</sup>
Aspect Ratio	2.65
Airfoil Section (Upper)	NACA 4415
Airfoil Section (Lower Root)	NACA 4415
Airfoil Section (Lower Tip)	NACA 4421

### Wing

Root Chord	4 ft 6 in.
Tip Chord	1 ft 11.5 in.
Overall Span	27 ft 4 in.
Total Exposed Area	58 ft <sup>2</sup>
Total Equivalent Area	98 ft <sup>2</sup>
Incidence	8 deg
Dihedral	10 deg
Quarter Chord Sweep	10 deg 45 min
Taper Ratio (Exposed)	0.44
Aspect Ratio (Overall)	8.0
Airfoil Section	NACA 4412

### Propulsion System

Engines	Two T58-GE-5
Takeoff Power (each)	1500 hp
Military Power	1400 hp
Normal Power	1250 hp
Transmission Rating	2800 hp

### Loading Conditions

Empty Weight	10,900 lb
Maximum Gross Weight Flown	18,000 lb
Maximum Gross Weight Capability	22,000 lb
Center-of-Gravity Range	258 in. to 276 in.

For simulation purposes, the loading condition and inertias used were as follows:

G.W.	14,800 lb
C.G.	276 in.
$I_x$	7800 slug-ft <sup>2</sup>
$I_y$	59,000 slug-ft <sup>2</sup>
$I_z$	53,000 slug-ft <sup>2</sup>
$I_{xz}$	3300 slug-ft <sup>2</sup>

Fuselage aerodynamic data used in the simulation were based on a 1/12 scale model test performed in the United Aircraft Corporation (UAC) 4 ft x 6 ft pilot tunnel and are presented in Figures 6 through 8. These data are from Reference 1. Rotor blade aerodynamic data were based on two-dimensional wind tunnel data taken in the 18-ft UAC main tunnel with the appropriate test section modifications. These data are shown in Reference 2.

The simulation was performed on a PDP-10 hybrid computer complex. The simulation, done in real time, had the following capabilities:

- a) Six fuselage degrees of freedom
- b) Nonlinear fuselage aerodynamic data
- c) Five blades, each with feathering and flapping degrees of freedom
- d) Nonlinear rotor blade airfoil section aerodynamic data with stall and Mach number effects

Flight data were recorded with an on-board tape system and reduced by digital computer. Simulation data were recorded on an analog time history plotter and an on-line typewriter.

## TEST PROCEDURES

Constant-speed turns to maximum achievable load factor were made both at ~~constant altitude and in descending flight.~~ In each case, load factor was increased until a power limit or a structural limit was reached. The power limit used was 2800 hp at 686 ft/sec rotor tip speed. The structural limit that defined most of the maneuver envelope was a rotor control load limit (1200 lb). This level of vibrating servo load is below the servo endurance limit, but it was selected to match the auxiliary control system capacity and to provide safety in the event of a primary control system malfunction. Turns were repeated with several stabilator bias angles to determine the effect of bias angles on load factor capability.

Symmetrical pull-ups were performed at various fixed collective settings, using longitudinal cyclic pitch to pull load factor. Again, rotor control loads were monitored to define the limits of the maneuver envelope.

Static lateral-directional stability, wings on and off, was measured in steady, level flight and steady sideslip of up to  $\pm 10$  degrees. Dynamic stability was measured by disturbing the aircraft from steady, level flight with longitudinal cyclic, lateral cyclic, and pedal pulses. These tests were run at aft C.G., the critical condition for dynamic stability evaluation.

Roll reversals were flown with and without wings, with nominal 2-inch lateral inputs, to define wing damping effects. Both directions were evaluated.

All tests were flown at 3,000 ft density altitude.

All tests were performed without stability augmentation, and no artificial force or control feedbacks were operational.

## RESULTS AND DISCUSSION

### LOAD FACTOR CAPABILITY

#### Results

Typical data in steady turns at light gross weight, aft C.G. are shown in Figure 9 at airspeeds of 100, 140, and 180 knots calibrated airspeed. Faired lines represent data for all stabilator bias angles. At 140 knots, for example, achieved load factors were 1.6 in a level turn and 2.4 in descent. Figure 10 summarizes these data and the load factors reached in symmetrical pull-ups in the conventional load factor-airspeed (V-g) format and illustrates the effects of maneuver condition and stabilator bias angle. The maneuver conditions are discussed in detail below. Little change in load factor capability was found when the bias angle was changed from the 2.5-degree angle found to be optimum in Reference 3.

A typical time history of a symmetrical pull-up is shown in Figure 11. Figure 12 shows control positions and engine torque at the point of maximum load factor with corresponding pull-up load factor at speeds of 140, 180, and 200 knots calibrated airspeed. Faired lines represent data for all stabilator bias angles.

Data at 17,300 lb gross weight for aft (276 in.) and forward (258 in.) C.G. locations are presented in Figures 13 through 15. Figure 13 shows representative results in turns at 180 knots. Figure 14 gives V-g results at aft and forward C.G. for turns and pull-ups. Figure 14 shows that load factor capability is higher at aft C.G. by approximately 0.15 g. The effects of C.G. location in level flight are shown in Figure 15. No change in power-limited maximum speed resulted from C.G. changes, but higher control system loads were observed at forward C.G., where more of the lift is carried on the rotor.

The summary of load factor data obtained by the S-67 with wings removed is shown in Figure 16. Faired lines from Figure 10 (with wings) are shown for comparison. Level flight characteristics with and without wings are compared in Figure 17.

#### Effect of Rotor Torque

Throughout these tests (see Figures 9, 12, and 13), higher load factors were achieved at lower values of collective pitch and rotor torque. This trend is predicted theoretically, for example in Reference 2, and the data from the current study have been examined to quantify the effect. Load factors achieved at 0, 40, 80 and 111% torque levels in turns and pull-ups at 14,800 lb gross weights are presented in Figure 18, where the data are taken from Figures 9 and 12. Two significant results are apparent. In either turns or pull-ups, load factor capability is strongly dependent on torque level. A difference of 1 g is typical over the range from zero to 100% torque. Secondly, for a given torque, airspeed, and gross weight, a greater load factor is achievable in a pull-up than in a steady turn at

speeds above about 150 knots. The difference is greatest at low torque levels where, in a pull-up, the rotor speed increases slightly (3 - 4%) with the result that lift capability increases. The fact that rotor speed is increasing also means that rotor shaft torque is greater than the aerodynamic torque being applied to the rotor (by as much as 10% power in pull-ups). The remainder of the difference in capability appears to be due to the transient nature of the local aerodynamic environment in the pull-up. The time history in Figure 11 shows that peaks of load factor, pitch rate, and other parameters are not occurring at precisely the same time. These variations in phasing may be the source of a part of the higher load factors produced at high speed in pull-ups.

#### Effect of Gross Weight

The effect of gross weight on load factor capability can be seen by comparing Figures 10 and 14. A 17% increase in gross weight resulted, on the average, in a 30% reduction in load factor capability. In other words, the product of  $g$  times gross weight was not constant, but increased with decreased gross weight. It is generally recognized (Reference 4) that rotor stall is delayed by the gyroscopic moments produced with positive aircraft pitching velocities. Since lighter gross weight results in higher load factors and higher pitch rates for the same rotor thrust, more stall alleviation results at light weights than at heavy weights. On the basis of these tests at two gross weights, the total lift capability is increased approximately 2% for each deg/sec of pitch rate.

#### Effect of Wings

In level flight, the primary effect of the wings on the S-67 (Figure 17) was to unload the rotor and to reduce rotor control system loads. In addition, the power-limited speed was increased slightly (2 - 4 knots) since rotor drag rise was alleviated.

The major effect of wings was to increase maneuver capability. Data for corresponding conditions in turns and symmetrical pull-ups are compared in Figure 19. Load factor capability is increased directly by the wing lift, and the higher load factors and associated higher pitch rates result in increases in rotor capability. For the S-67, these two effects are of the same order of magnitude. An approximate breakdown of the load factor differences in Figure 19 is given in Table III. The lift increase due to pitch rate has been estimated on the basis of the results at different gross weights, as discussed in the preceding section. At 100 knots, pitch rates are high, and wing effectiveness is greatly increased by rotor stall alleviation. At 180 knots, most of the lift increase with wings on comes from lift of the wing itself.

The useful maneuver capability derived from flight data and encompassing the effects of changes in stabilator bias angle and aircraft center of gravity as well as gross weight, airspeed and rotor torque is summarized in Figure 20. Load factors up to the levels shown can be sustained for a second or more without structural damage or significant deterioration of handling qualities.

The pilot technique necessary to achieve the desired maneuverability in a winged helicopter, with a minimum loss in airspeed and/or altitude, is to apply aft cyclic pitch and lower the collective pitch (and hence, torque) as required to limit the control system loads. The S-67 control loads may be monitored on the cruise guide indicator. Alternatively, control loads may activate a collective stick shaker, as investigated and reported subsequently in Reference 5 (pages 14-16).

TABLE III. DERIVATION OF MANEUVER LEAD DISTRIBUTION

Aircraft (K-43)	Ave P, Wings on	Total Lift (lb)	Ave P, Wings off	Total Lift, Wings off (lb)	Change in Pitch Rate, $\dot{\theta}_f$ (deg/sec)	$\Delta$ Lift Due to $\dot{\theta}_f$ (lb)	$\Delta$ Lift Wings/Poly (lb)	$\frac{\Delta \text{ Lift}}{\text{Wings/Poly}}$
100	1.0	24,000	1.0	20,000	5.3	5	5	1
140	1.0	30,000	1.05	21,750	5.8	15.9	15.9	1.5
180	1.0	36,000	1.03	18,200	5.3	1000	1500	1.5
<p>Ave T.W. = 14,500 lb</p> <p>Ast C.G. = .70 in.</p>								

## AIRCRAFT STABILITY

### Longitudinal Dynamic Stability

Longitudinal dynamic stability characteristics of the S-67 were evaluated at airspeeds of 100, 140, and 180 KCAS. The tests were conducted at aft C.G., the critical condition for dynamic stability evaluations. Figure 21 is a typical time history. Each test case was evaluated by measuring the period and time to half or double amplitude for the oscillatory envelope. These time histories can be represented by an equivalent linear equation of the form

$$\theta_f = e^{nt} (A \sin \omega t + B \cos \omega t) \quad (1)$$

a general solution of the differential equation

$$(I\ddot{\theta} + C\dot{\theta} + K)\theta_f = 0 \quad (2)$$

with the characteristic roots

$$\lambda_{1,2} = (n \pm j\omega) \quad (3)$$

These roots define stability characteristics. Negative  $n$  is stable and positive  $n$  is unstable;  $\omega$  is the frequency of the airframe oscillation. Using the flight test time histories, the real portions of the roots were derived by the formula  $n = -\ln 2/\text{time to half amplitude}$  and  $n = \ln 2/\text{time to double amplitude}$ . The imaginary portions of the roots were derived by the formula  $j\omega = 2\pi/\text{time period of one cycle}$ .

Figure 22 summarizes the results of this analysis and includes the requirements of MIL-H-8501A (Reference 6). At low speeds, the longitudinal characteristics were slightly unstable, but the period of oscillation was long, so the longitudinal dynamic stability of the S-67 without stability augmentation meets or exceeds the IFR requirements of Reference 6 from 100 KCAS to  $V_{\text{max}}$ .

### Lateral-Directional Stability

Static lateral-directional characteristics of the S-67 are shown in Figure 23. At 140 KCAS, wings on, the pedal slope is 4.2%/deg sideslip. Wings off, the pedal slope is 1.82%/deg. The basic S-61 (Reference 7) has a pedal slope of 0.125%/deg at 128 KCAS. The low sponson arrangement, combined with the large fuselage side area, provides a very shallow lateral stick slope of 0.30%/deg. Wings off, the stick slope is 0.40%/deg. The 10° dihedral of the wings just compensates for their low waterline location. The basic S-61 has a lateral stick slope of 0.75%/deg. The large vertical fin of the S-67 improves the directional stability over earlier S-61 type aircraft, as demonstrated by the strongly positive pedal position slope. Lateral and directional dynamic characteristics of the S-67 are satisfactorily damped. Figures 24 and 25 are typical time histories at 140 KCAS,

and Figure 26 is a summary of derived characteristic roots. Without stability augmentation, the S-67 lateral-directional stability also meets or exceeds the IFR requirements of Reference 6 from 100 KCAS to  $V_{max}$ .

Lateral control reversals with  $\pm 45^\circ$  roll showed that maximum roll rates meet the requirements of Reference 8, even with the wings on. Figures 27 and 28 are typical roll reversal time histories with and without wings. Roll rate vs lateral stick is plotted for various airspeeds in Figure 29.

### SIMULATION STUDIES

The Sikorsky hybrid simulator was used to evaluate control system changes that might improve S-67 maneuverability characteristics. Figures 30 through 36 show the results. A correlation of flight characteristics was performed in the Reference 3 test program. No additional simulator changes were required for this study. Comparisons of flight test results and computer simulation results are included in Figures 31 (effect of bias angle at 2800 hp), 35 (effect of power), and 36 (effect of lateral cyclic). Additional maneuver data point comparisons were not available because the analysis was performed at the upper limit of 2800 hp, rather than at the lower control load limits.

Variations in longitudinal control coupling and differential feedback to the stabilator were examined for improved rotor/wing load sharing. Table II lists the variations evaluated. Constant-power 180-KCAS descending turns were used to evaluate all control system variations.

Control coupling variations had little effect on load sharing; see Figure 30. Bias angle changes (Figure 31) and feedback of load factor or pitch rate to the longitudinal control (Figures 32, 33 and 34) also had little effect. Variation in power setting (Figure 35) showed marked effect on load sharing. This result is in agreement with flight tests, in which higher load factor capability was demonstrated at lower collective pitch and rotor torque.

S-67 roll characteristics were evaluated in a manner similar to the flight tests. Control inputs were used to evaluate roll control sensitivity with and without differential speed brake actuation. As expected, roll control improves with the coupling of the speed brakes as spoilers. Because only lift reduction is available, the use of spoilers is not as beneficial to aircraft performance as ailerons would be. However, in light of the other benefits of wing-mounted speed brakes (Reference 9), there is a definite advantage in using the existing control surfaces for roll control improvement.

The results of the differential speed brake investigation are presented in Figure 36. Measurable control improvements are shown with the systems evaluated. A comparison with fixed-wing roll control specifications, Reference 8, is also shown. The comparison shows that differential speed brake control is not required for the S-67, but the concept does provide a simple way to provide added capability.

## CONCLUSIONS

Addition of wings to the S-67 helicopter improved maneuvering load factor capability by more than 50% at high speed. Control coupling variations had little effect on load sharing.

Rotor lift capability is greatest at low collective pitch and low rotor torque levels. Rotor contribution to total lift capability is increased at higher load factors because of the gyroscopic moments due to pitch rate. As a result, load factor sensitivity to gross weight changes or the addition of a wing is magnified.

Wings improve level-flight speed capability by delaying drag rise and control load buildup due to rotor stall.

Without AFCS at aft C.G. for all speeds above 100 KCAS, the S-67 configuration demonstrated dynamic stability characteristics equal to or in excess of MIL-H-8501A requirements.

Roll control capability is only slightly reduced by the S-67 wing configuration, and use of differential speed brakes can more than compensate for this change. The configuration tested showed no requirement for such a modification.

#### LITERATURE CITED

1. Gifford, J., ONE TWELFTH SCALE WIND TUNNEL TESTS ON THE AH-3 (S-67) DEMONSTRATOR AIRCRAFT, SER-67000, Sikorsky Aircraft Division of United Aircraft Corporation, Stratford, Connecticut, June 1970.
2. Tanner, W. H., CHARTS FOR ESTIMATING ROTARY WING PERFORMANCE IN HOVER AND HIGH FORWARD SPEEDS, SER-50379, U.S. Navy Contract NASw-745, Sikorsky Aircraft Division of United Aircraft Corporation, Stratford, Connecticut, August 1964.
3. Kaplita, T. T., INVESTIGATION OF THE STABILATOR ON THE S-67 AIRCRAFT, Sikorsky Aircraft Division of United Aircraft Corporation; USAAMRDL Technical Report 71-55, Eustis Directorate, U.S. Army Air Mobility Research and Development Laboratory, Fort Eustis, Virginia, October 1971, AD 735766.
4. Brown, E. L., and P. S. Schmidt, THE EFFECT OF HELICOPTER PITCHING VELOCITY ON ROTOR LIFT CAPABILITY, Journal of the American Helicopter Society, Vol. 8, No. 4, October 1963.
5. O'Conner, S. J., and D. W. Fowler, S-67 AIRCRAFT FEEL AUGMENTATION SYSTEM FLIGHT EVALUATION, Sikorsky Aircraft Division of United Aircraft Corporation; USAAMRDL Technical Report 72-41, Eustis Directorate, U.S. Army Air Mobility Research and Development Laboratory, Fort Eustis, Virginia, August 1972, AD 749284.
6. GENERAL REQUIREMENTS FOR HELICOPTER FLYING AND GROUND HANDLING QUALITIES, Military Specification MIL-H-8501A, U.S. Government Printing Office, Washington, D.C., April 1968.
7. Macomb, J., and A. Skarzynski, AERODYNAMIC DEMONSTRATION OF THE HSS-2 HELICOPTER FOR THE BUREAU OF NAVAL WEAPONS, SER-61414, U.S. Navy Contract NOa(s)58-208c, Sikorsky Aircraft Division of United Aircraft Corporation, Stratford, Connecticut, June 1961.
8. FLYING QUALITIES OF PILOTED AIRPLANES, Military Specification MIL-F-8785 (ASG), U.S. Government Printing Office, Washington, D.C., August 1969.
9. Kefford, N. F., INVESTIGATION OF SPEED BRAKES ON THE S-67 AIRCRAFT, Sikorsky Aircraft Division of United Aircraft Corporation; USAAMRDL Technical Report 72-22, Eustis Directorate, U.S. Army Air Mobility Research and Development Laboratory, Fort Eustis, Virginia, April 1972, AD 745214.

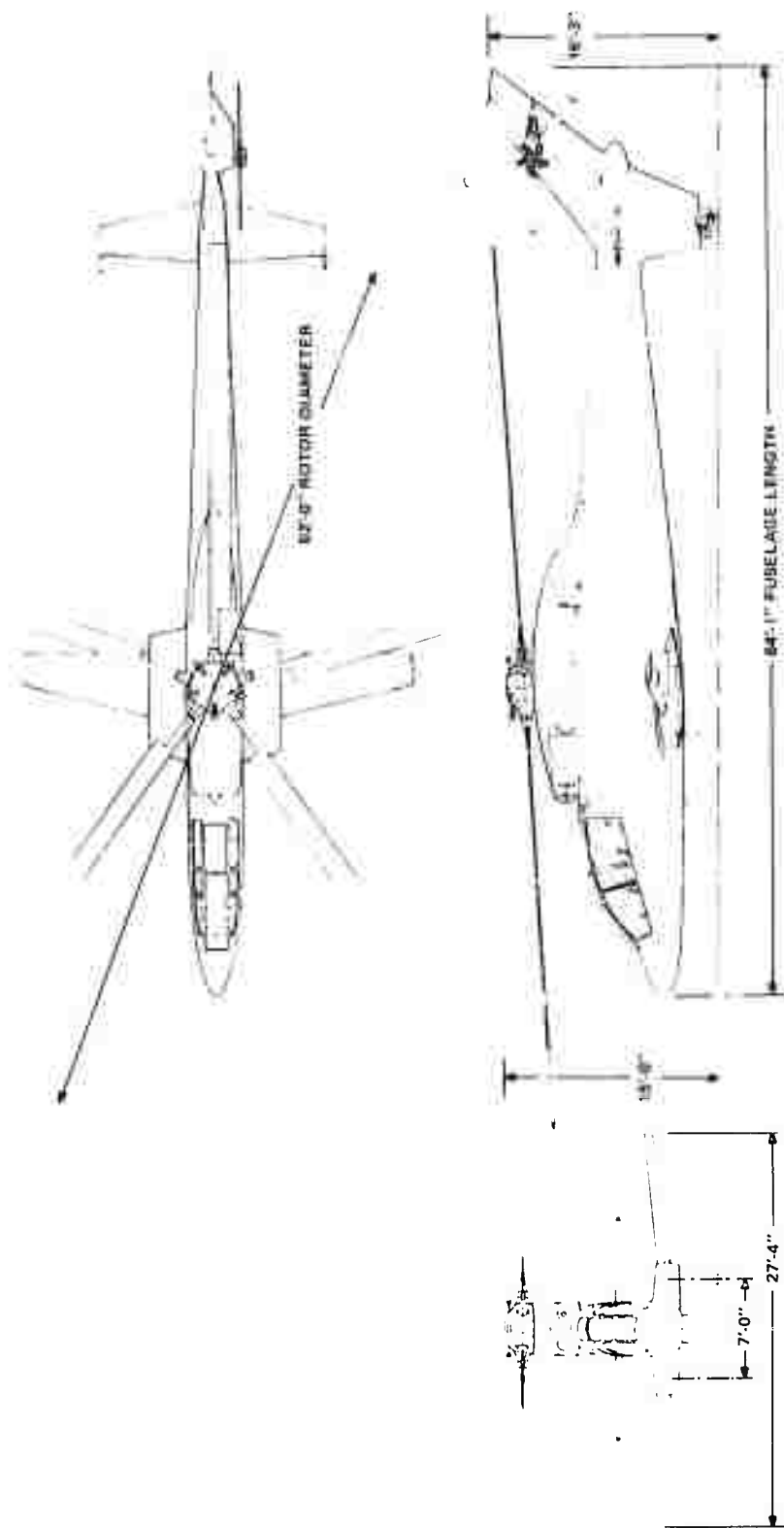


Figure 1. S-67 Three-View Drawing.



Figure 2. Small aircraft, in the foreground.

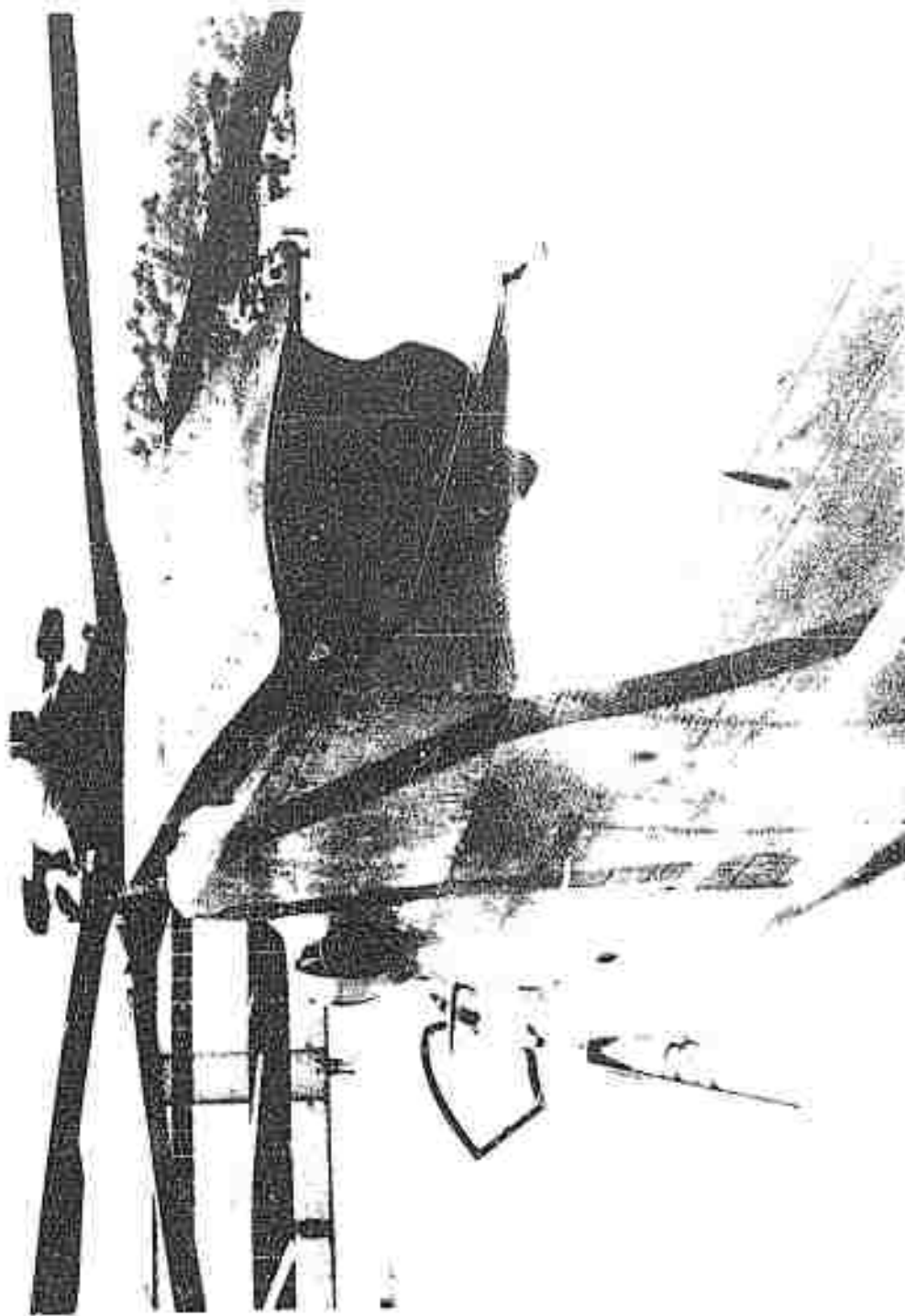
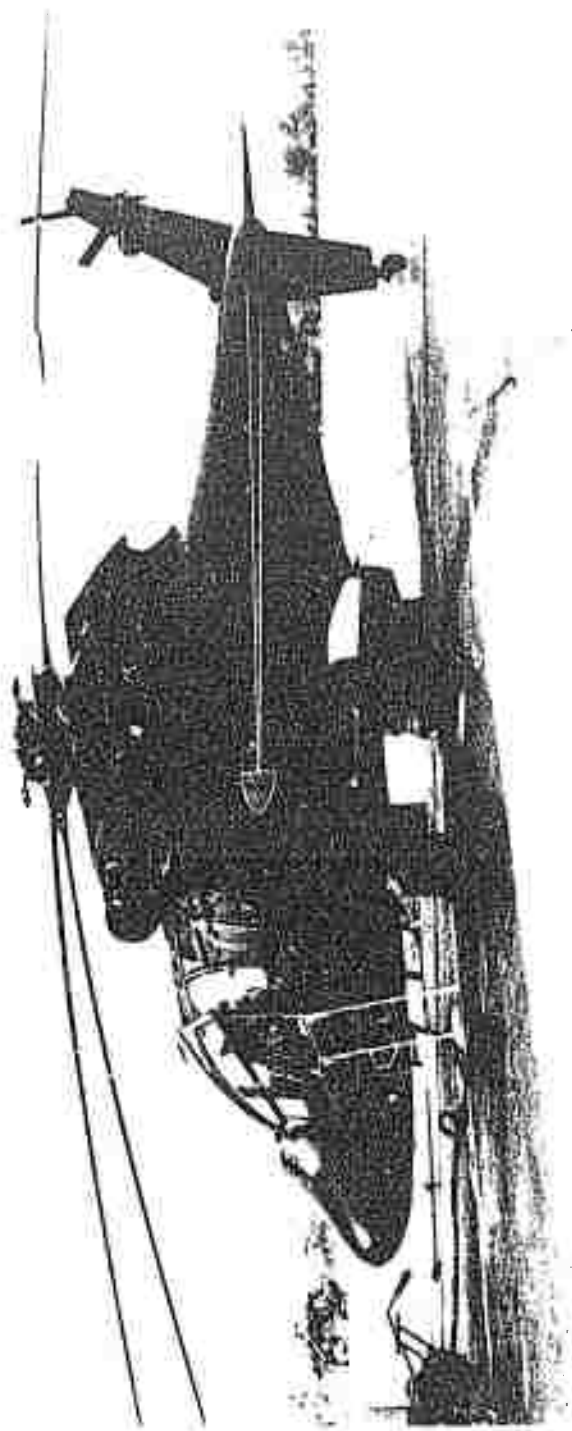


Figure 3. 3-6" Main Flow Inlet With Prototype Flow Separator.



SEARCHLIGHT AND GUN TURRET, DECK, U.S.S. ALBATROSS (AG-39)



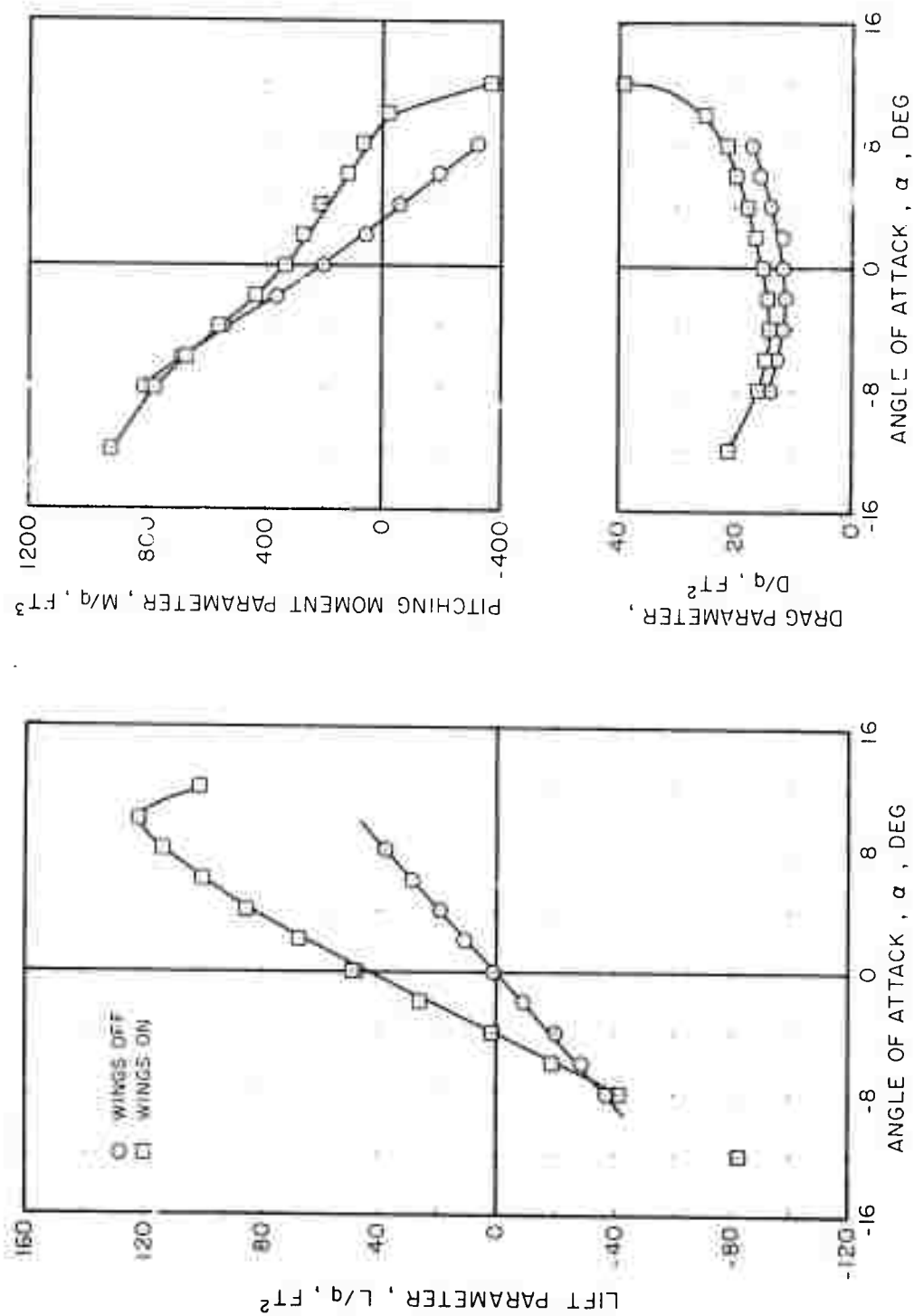


Figure 6. S-67 Wind Tunnel Data Showing the Effect of Wings on Lift, Drag, and Pitching Moment Parameters.

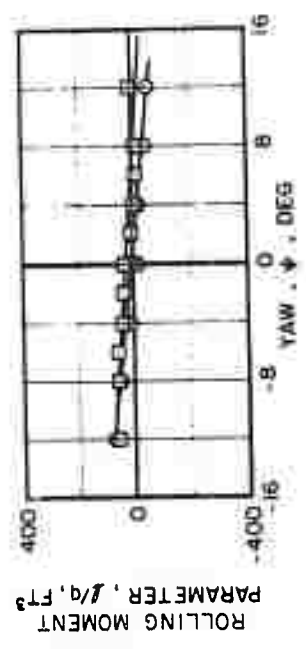
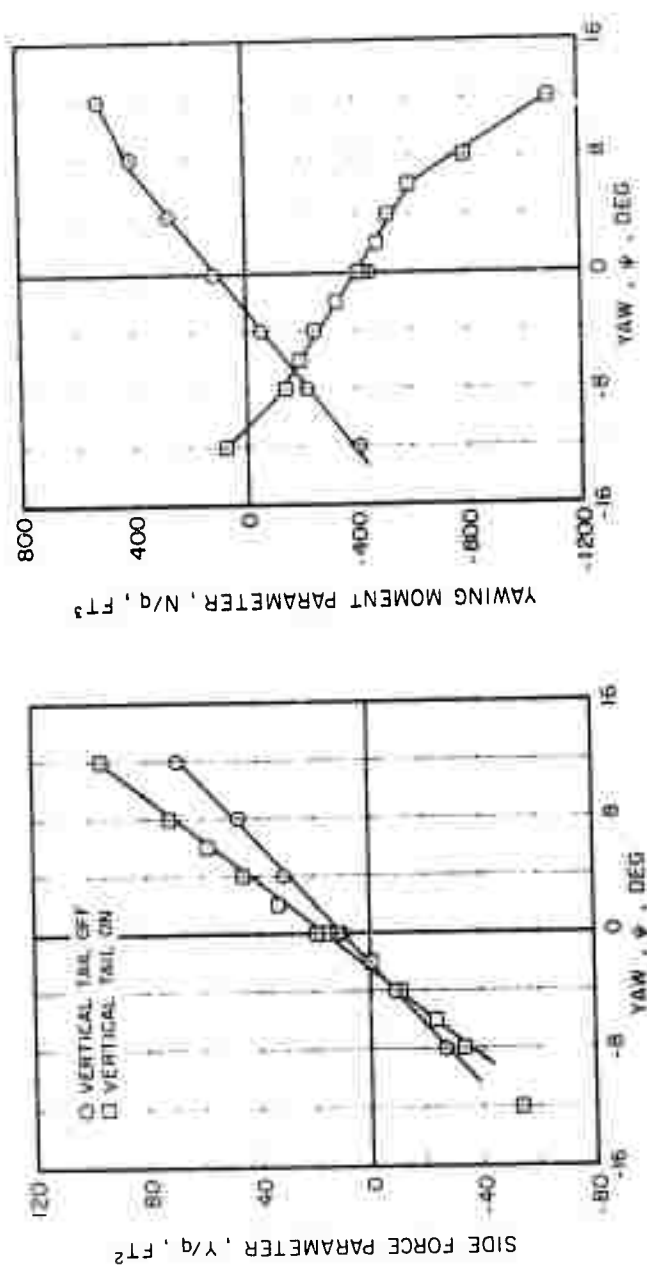


Figure 7. S-67 Wind Tunnel Data Showing the Effect of the Vertical Tail on Side Force, Yawing Moment, and Rolling Moment Parameters.

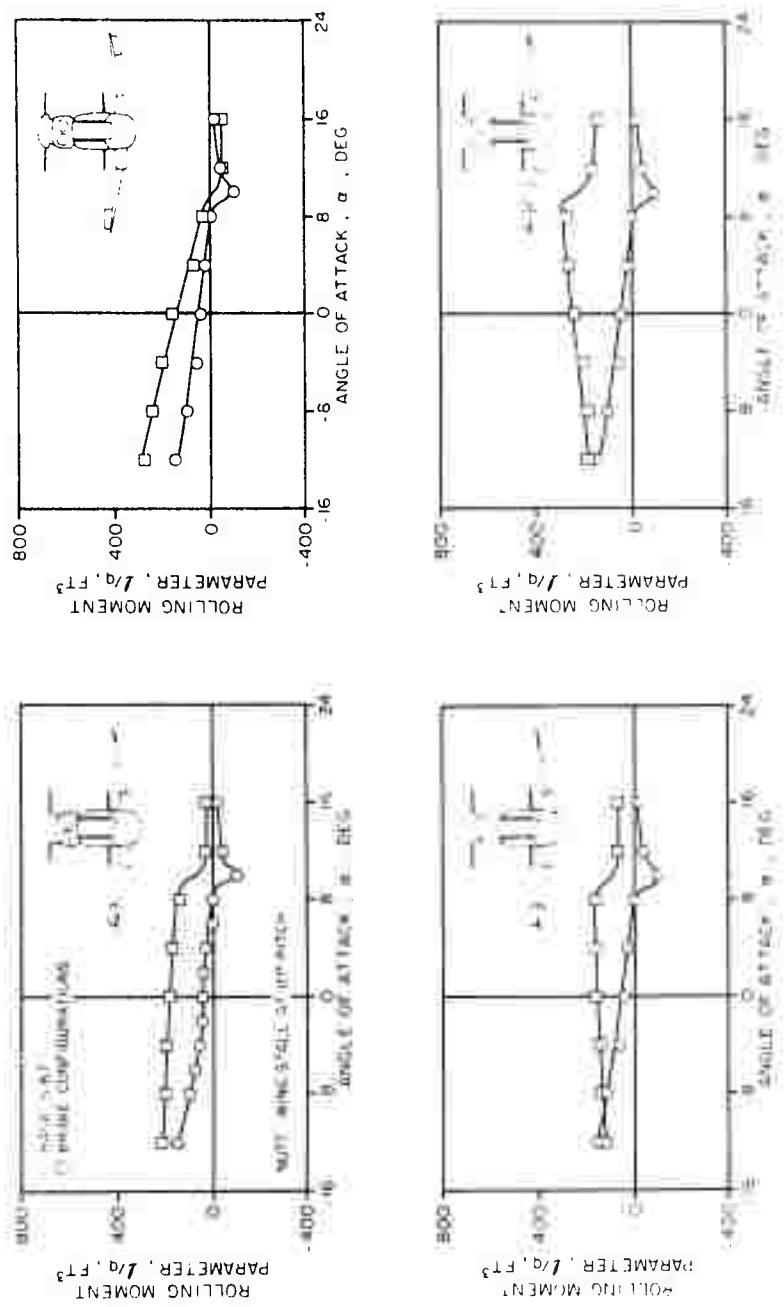
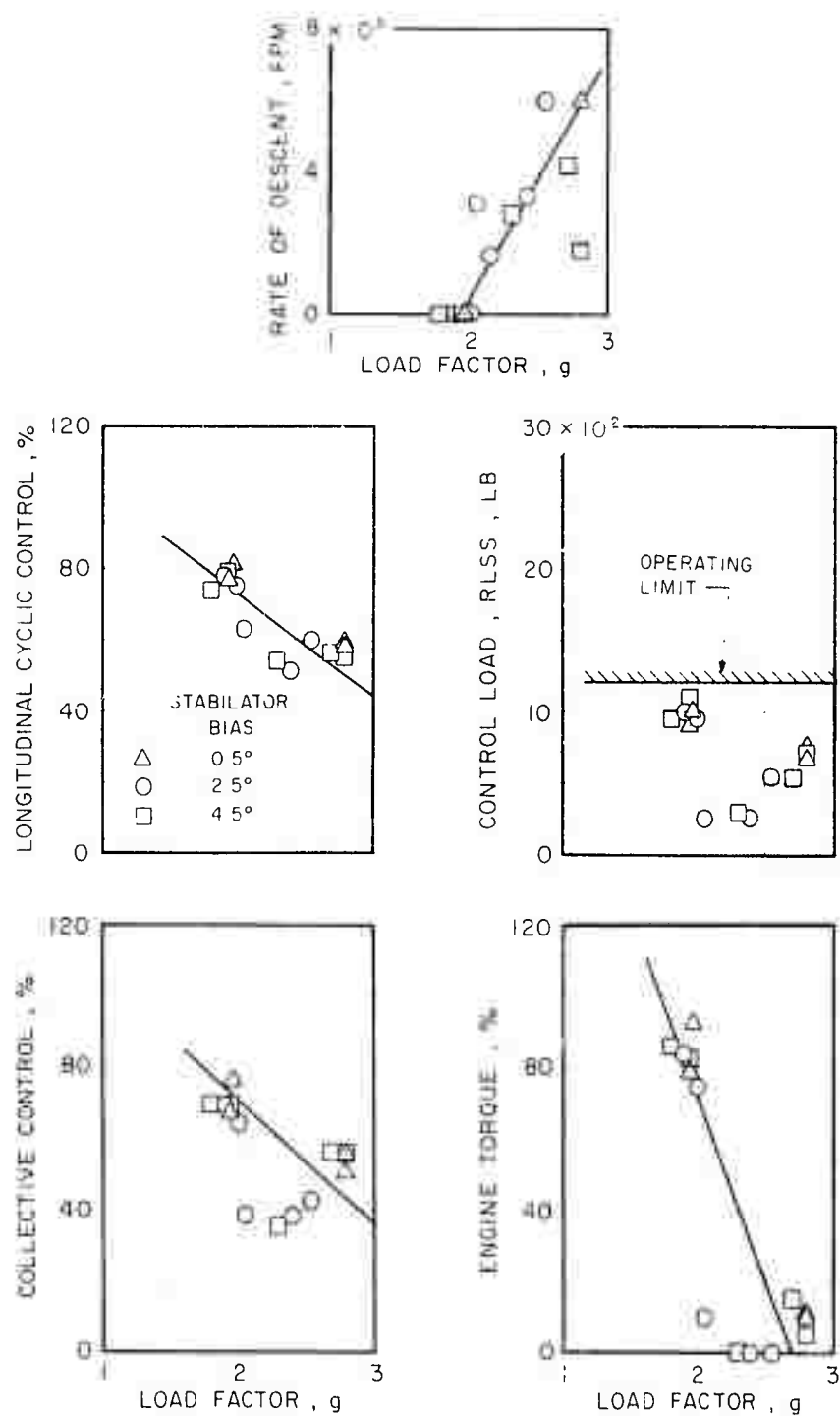
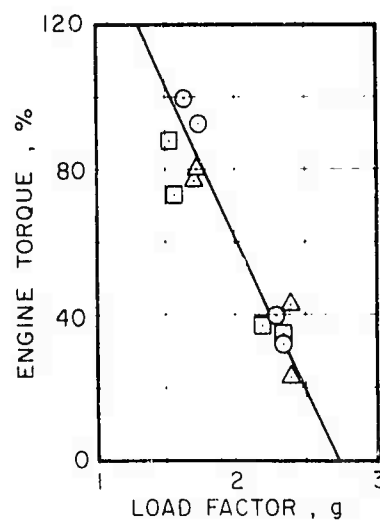
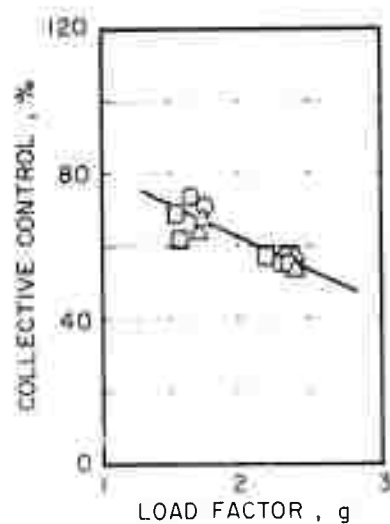
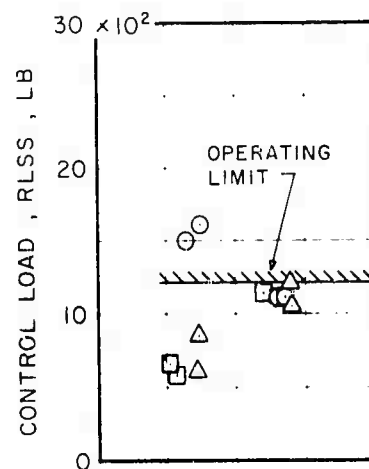
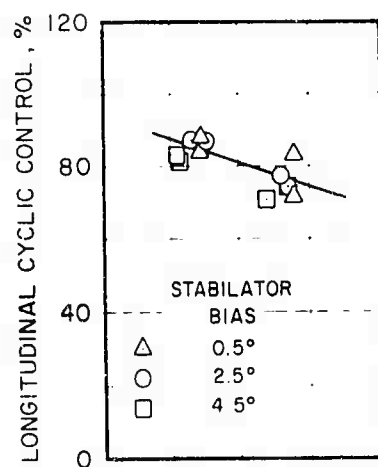
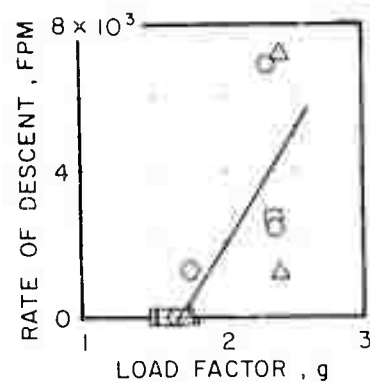


Figure 8. S-67 Wind Tunnel Data Showing the Effect of Various Speed Brake Combinations on Rolling Moment.



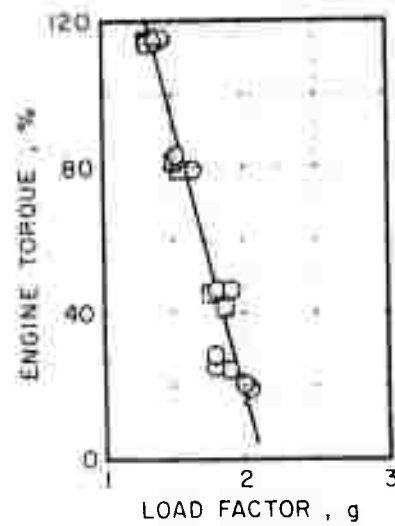
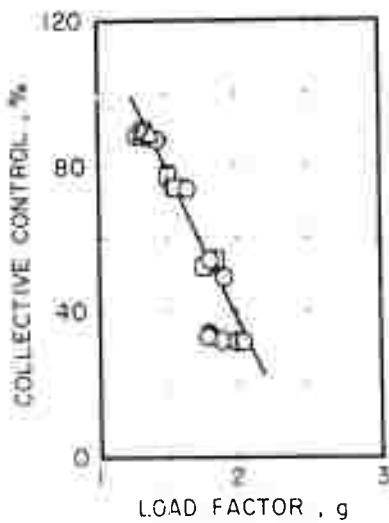
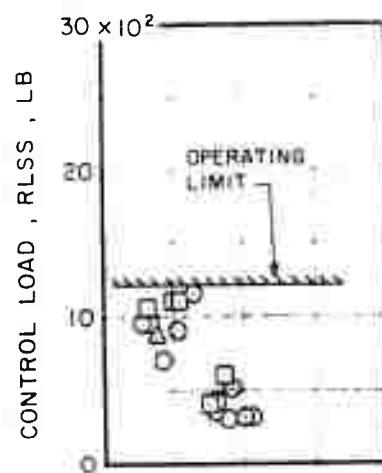
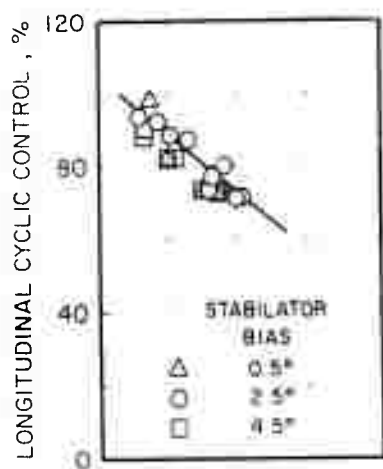
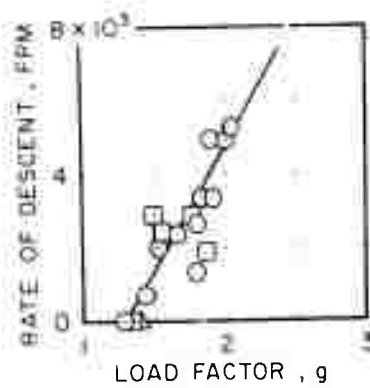
(a) V = 100 KCAS

Figure 9. S-67 Longitudinal Cyclic, Rate of Descent, Control Load, Collective, and Engine Torque vs Load Factor at 14,800 lb, 276 C.G. in Steady Turns.



(b)  $V = 140$  KCAS

Figure 9. Continued.



(c)  $V = 180$  KCAS

Figure 9. Concluded.

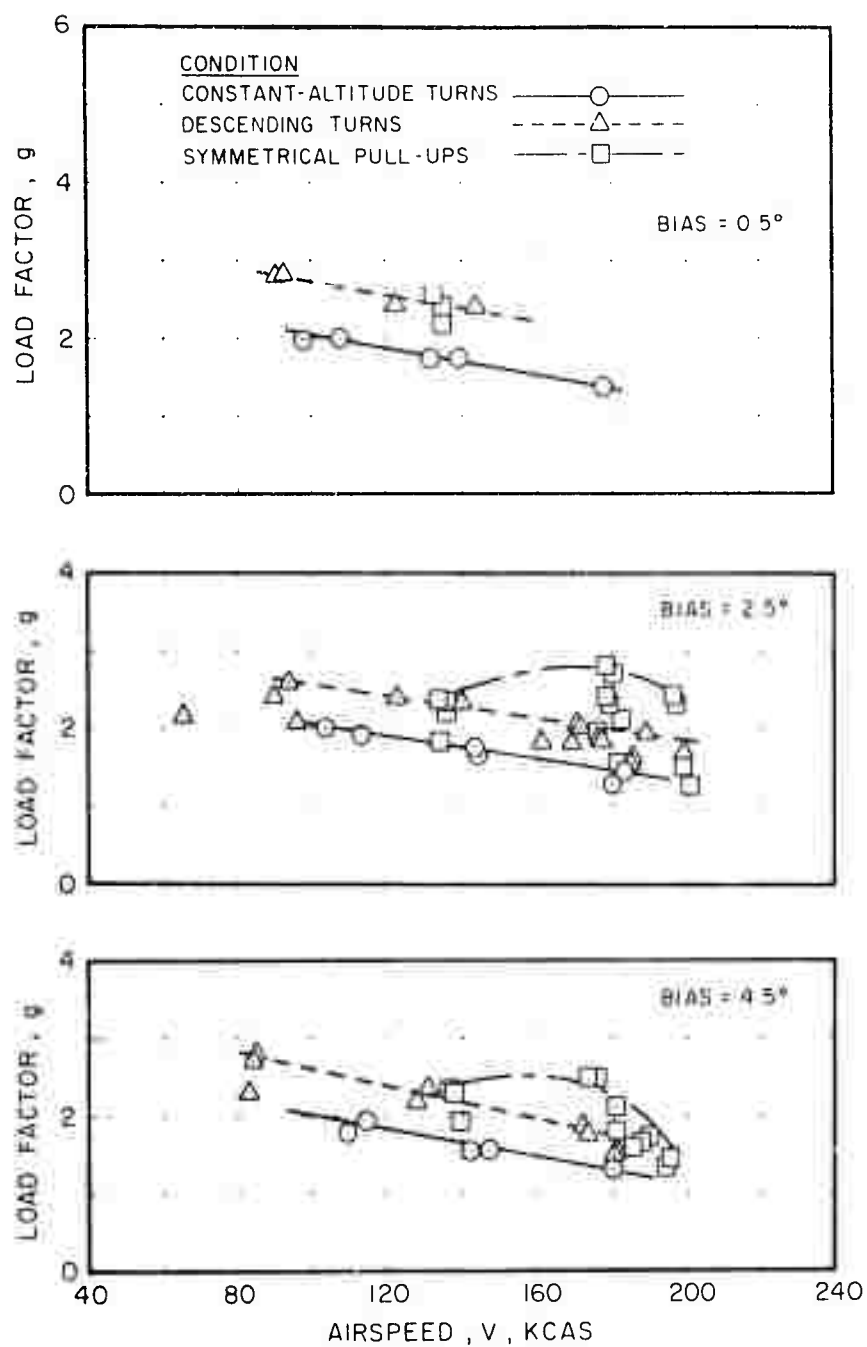


Figure 10. S-67 Summary of Load Factor Data vs Airspeed at 14,800 Lb, 276 C.G., Showing the Effects of Maneuver Condition and Stabilator Bias Angle.

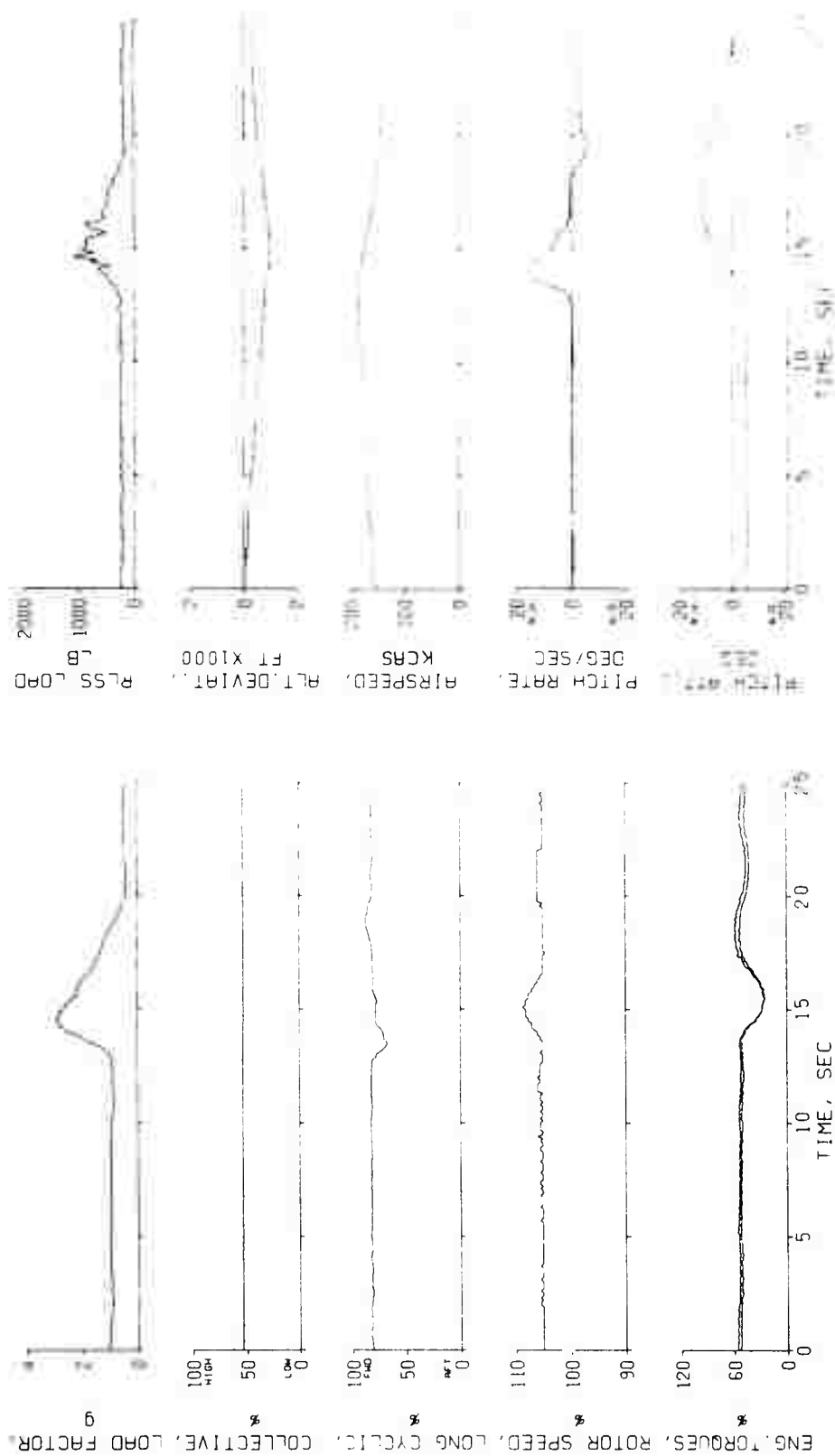
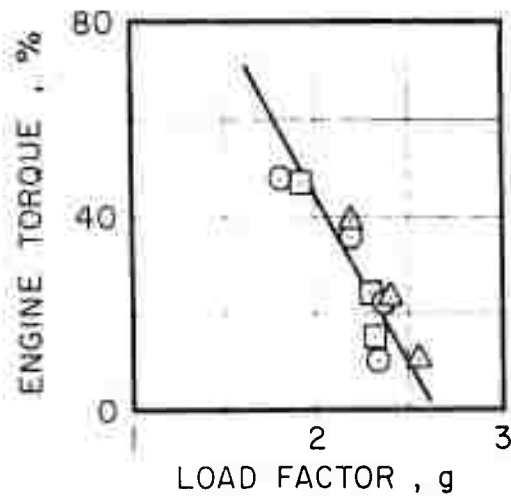
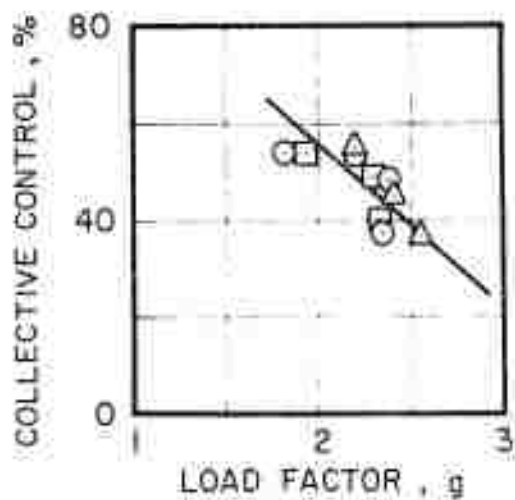
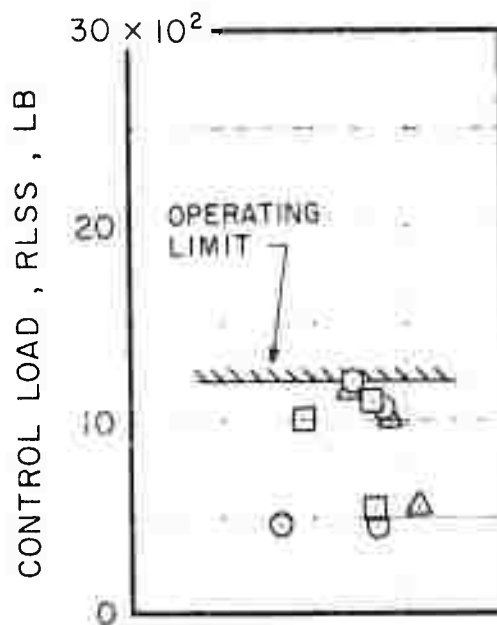
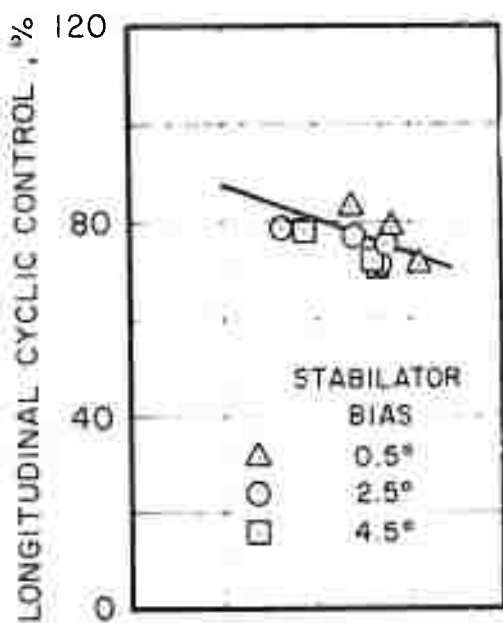
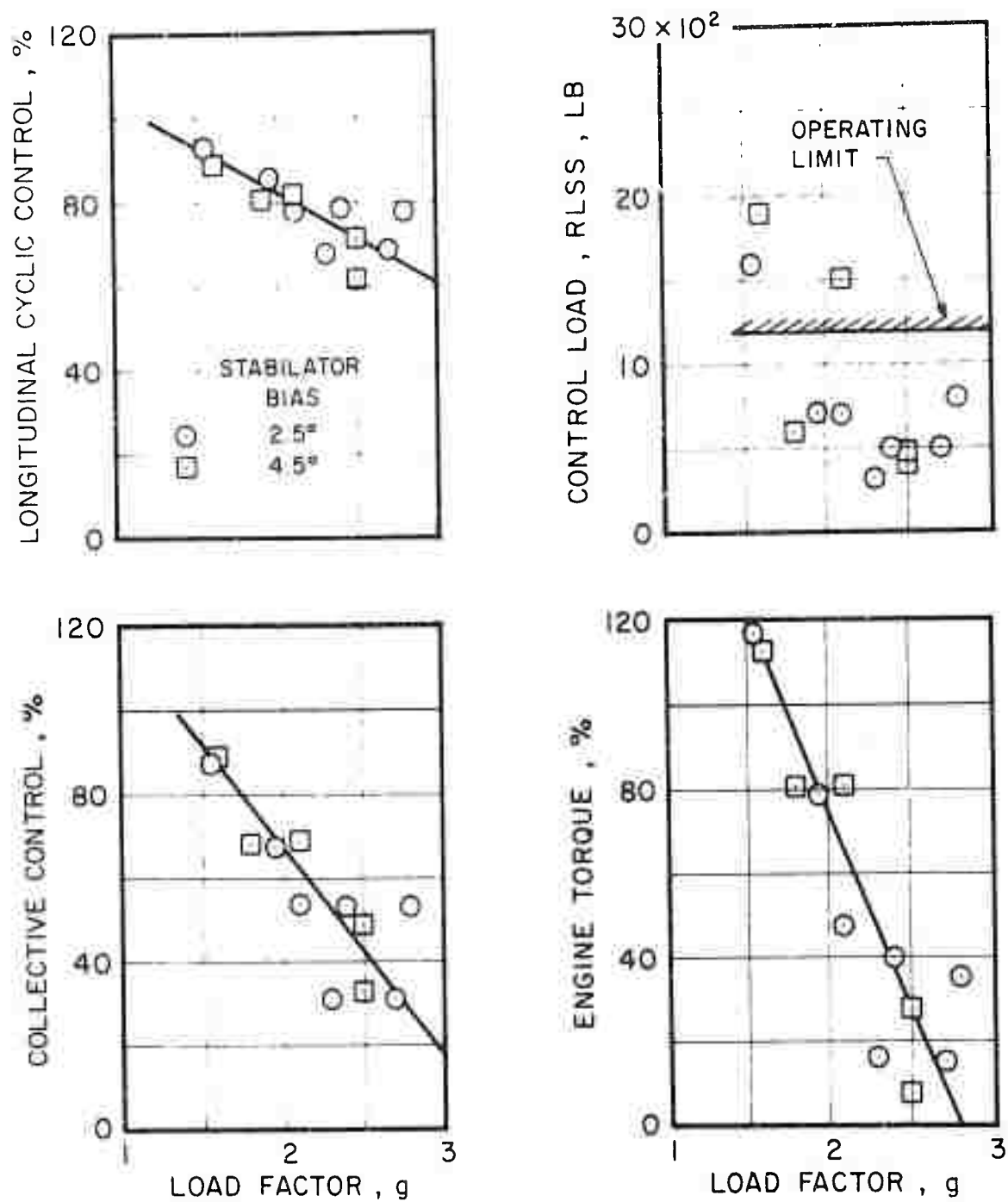


Figure 11. S-67 Symmetrical Pull-Up at 100 KIAS, 16,000 FT, 276 C.G., 0.5 Deg Stabilizer Trim.



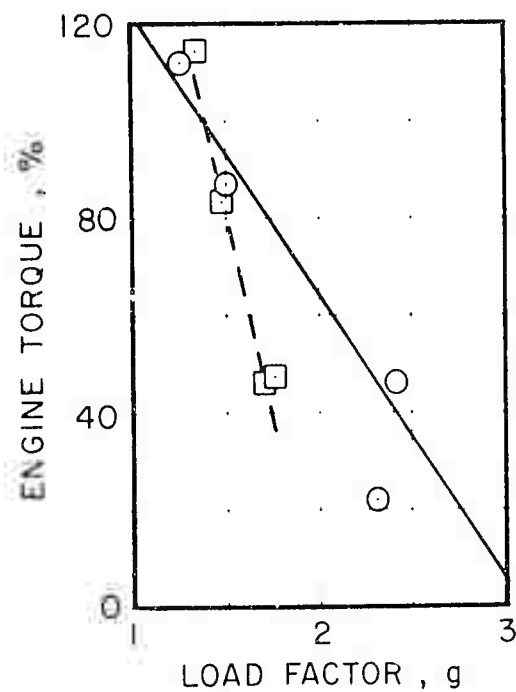
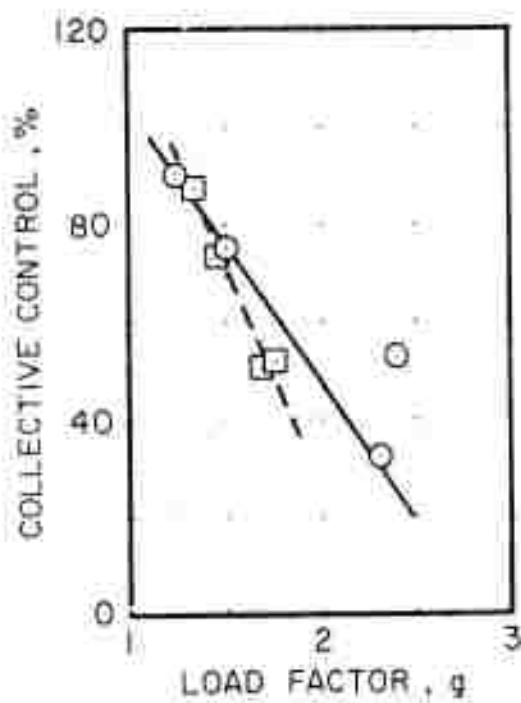
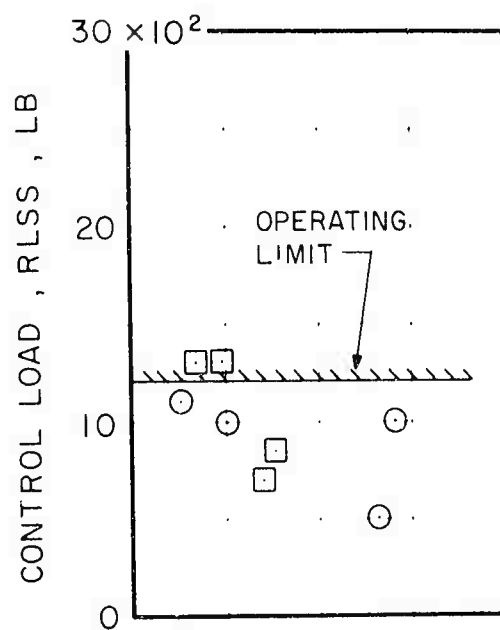
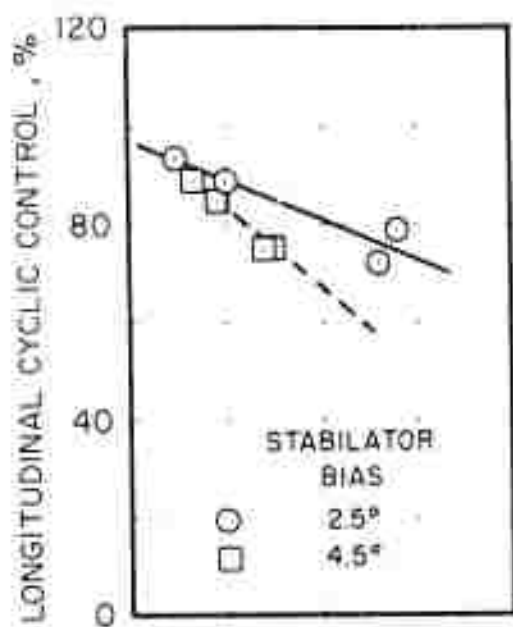
(a)  $V = 140$  KCAS

Figure 12. S-67 Longitudinal Cyclic, Control Load, Collective, and Engine Torque vs Load Factor at 14,800 Lb, 276 C.G. in Symmetrical Pull-Ups.



(b)  $V = 180$  KCAS

Figure 12. Continued.



(c)  $\gamma = 100 \text{ PERCENT}$

Figure 11. Concluded.

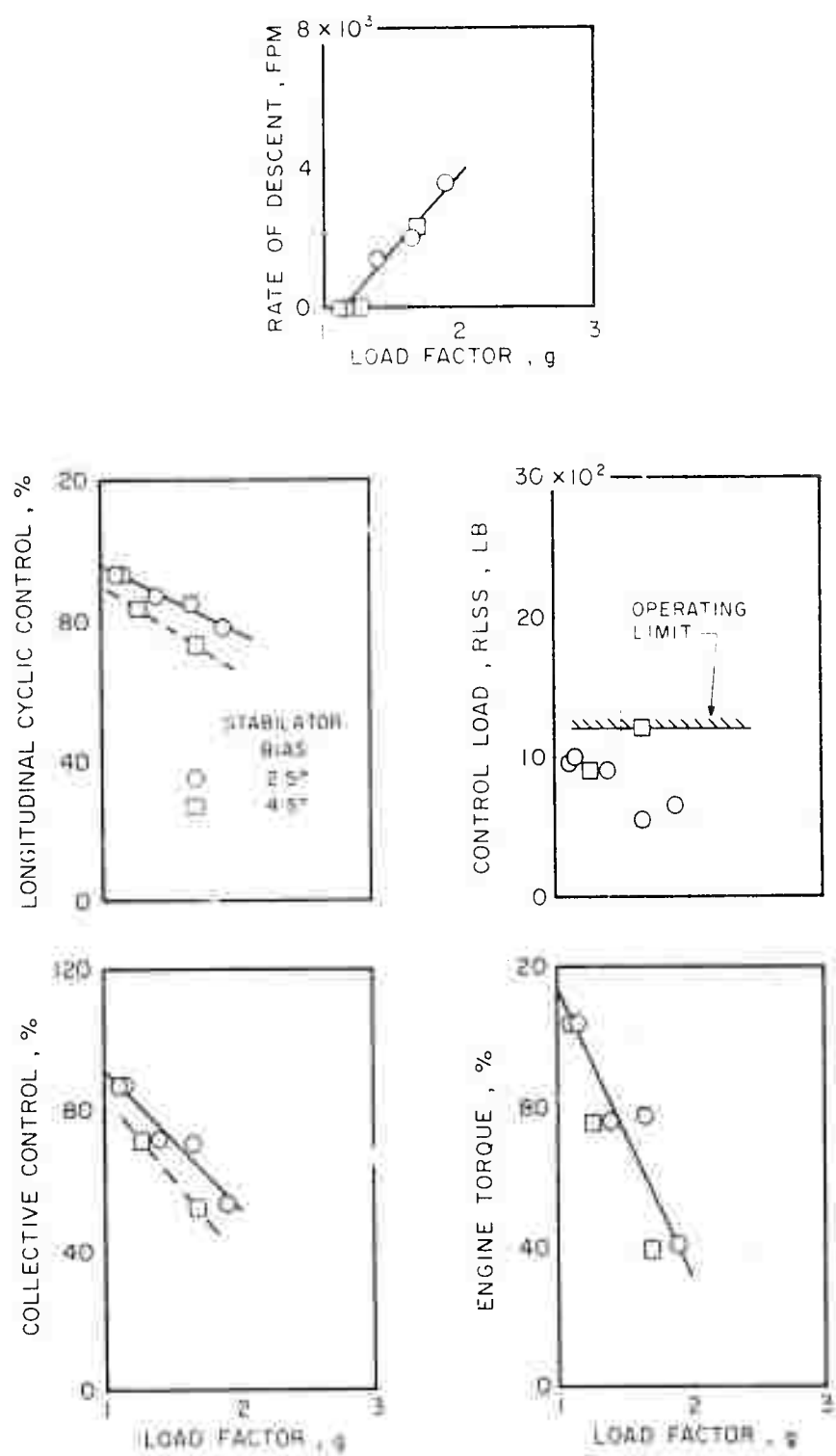
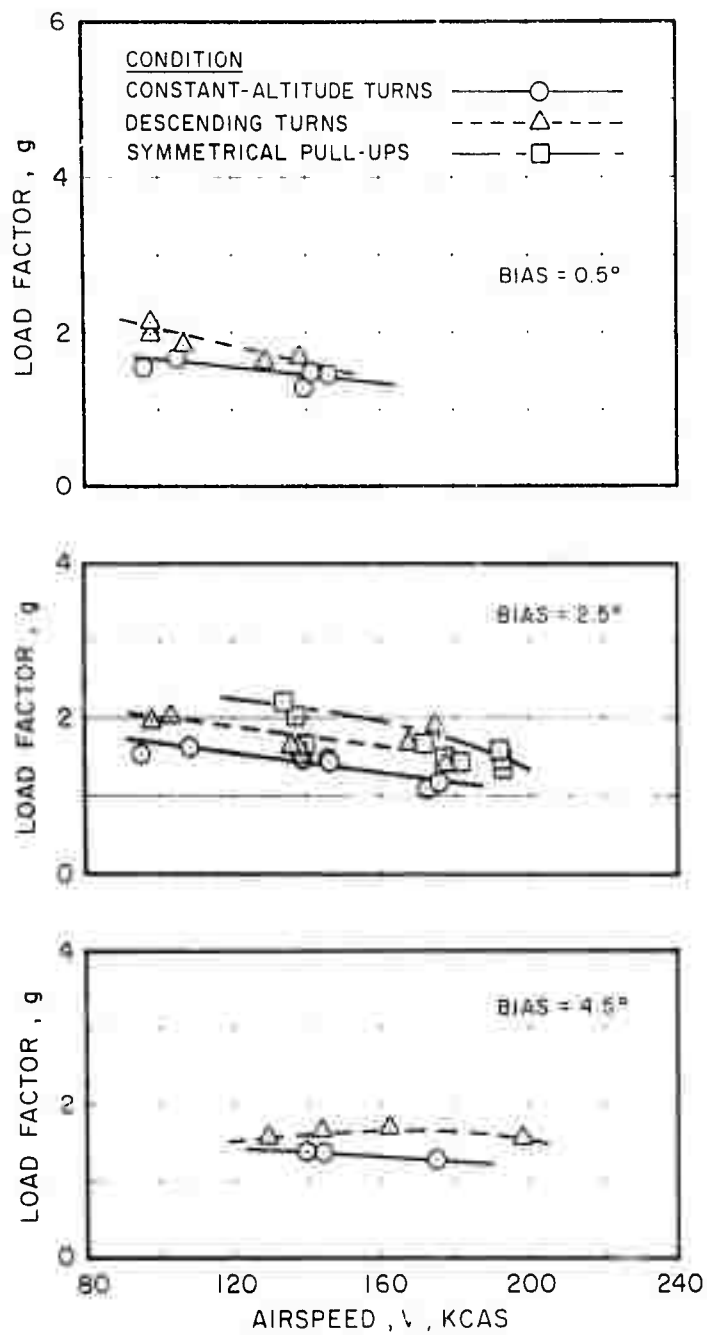
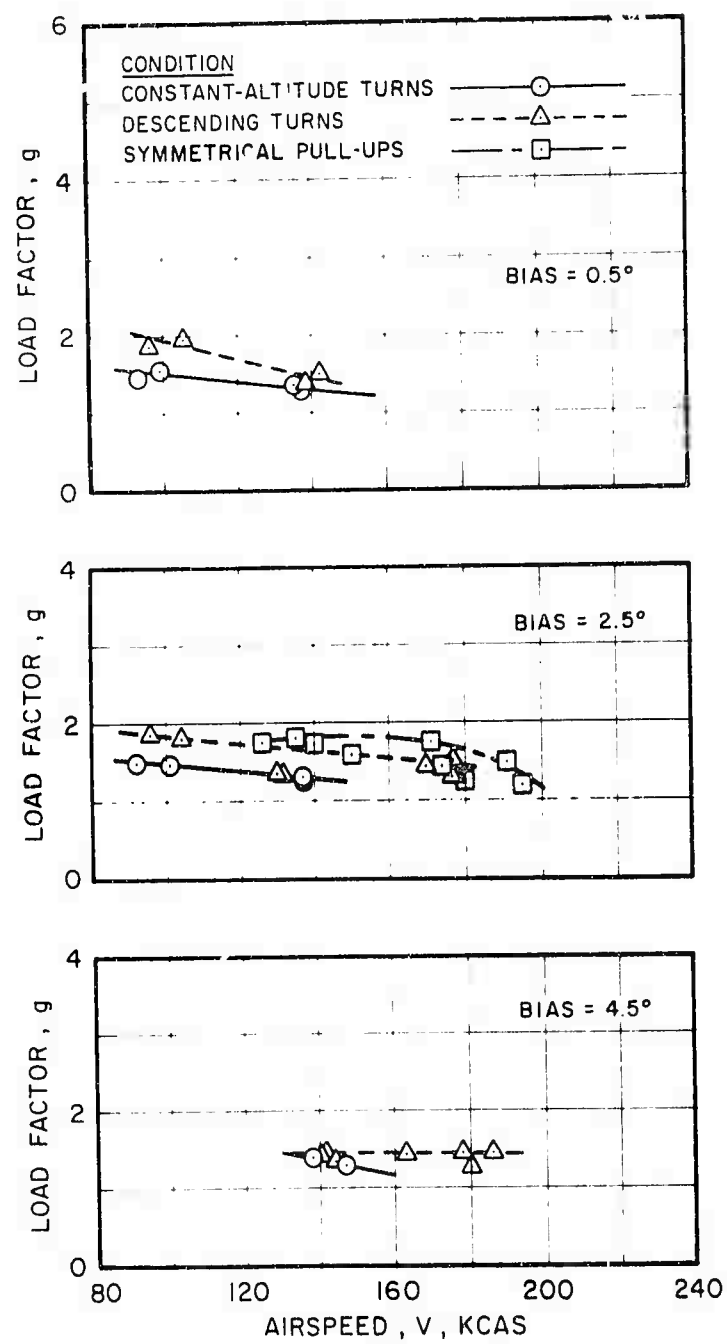


Figure 13. F-67 Longitudinal Cyclic, Rate of Descent, Control Load, Collective, and Engine Torque vs Load Factor at 17,300 Lb, 276 C.G., 180 KCAS in Steady Turns.



(a) C.G. = 276 in.

Figure 14. S-67 Summary of Load Factor Data vs Airspeed at 17,300 Lb, Showing the Effects of Maneuver Condition, Stabilator Bias Angle, and C.G.



(b) C.G. = 258 in.

Figure 14. Concluded.

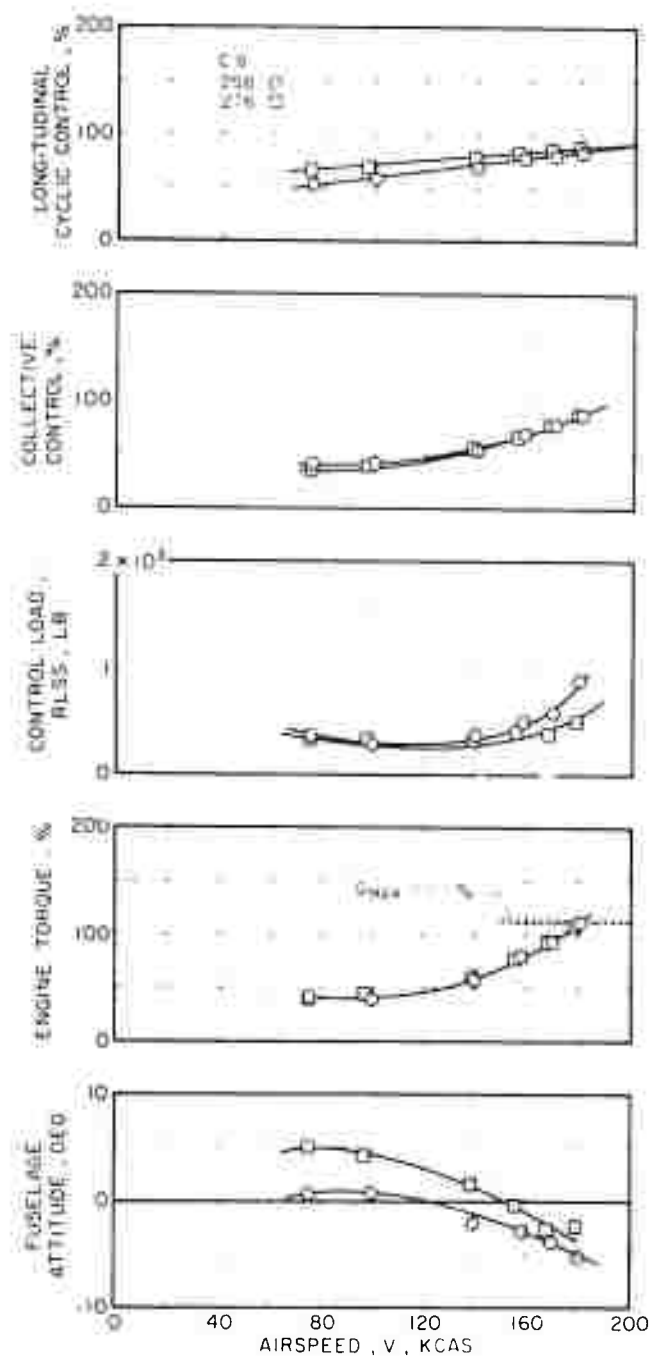


Figure 15. S-67 Comparison of Level-Flight Data at Forward and Aft C.G. at 17,300 Lb, 2.5 Deg Stabilator Bias Angle.

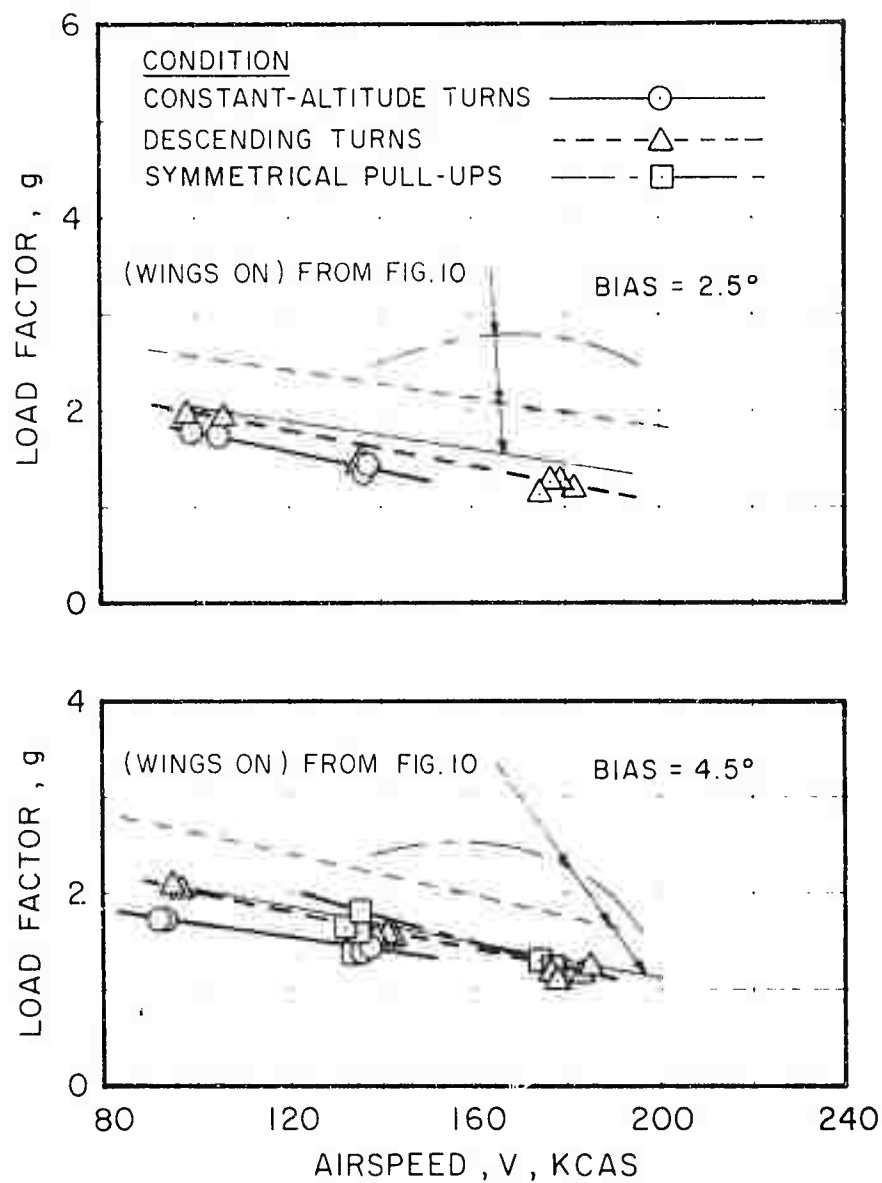


Figure 16. S-67 Summary of Load Factor Data vs Airspeed at 14,800 Lb, 276 C.G., Without Wings, Showing the Effects of Maneuver Condition, Wings, and Stabilator Bias Angle.

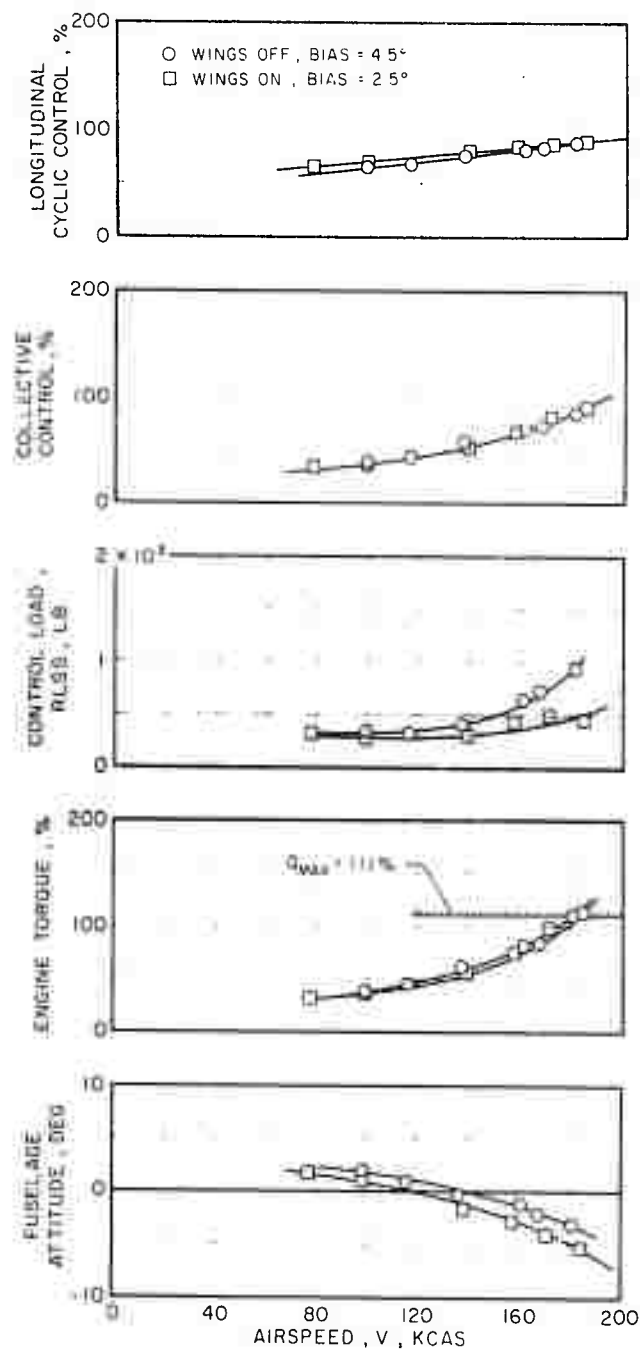


Figure 17. S-67 Comparison of Level-Flight Data With and Without Wings at 14,800 Lb, 276 C.G.

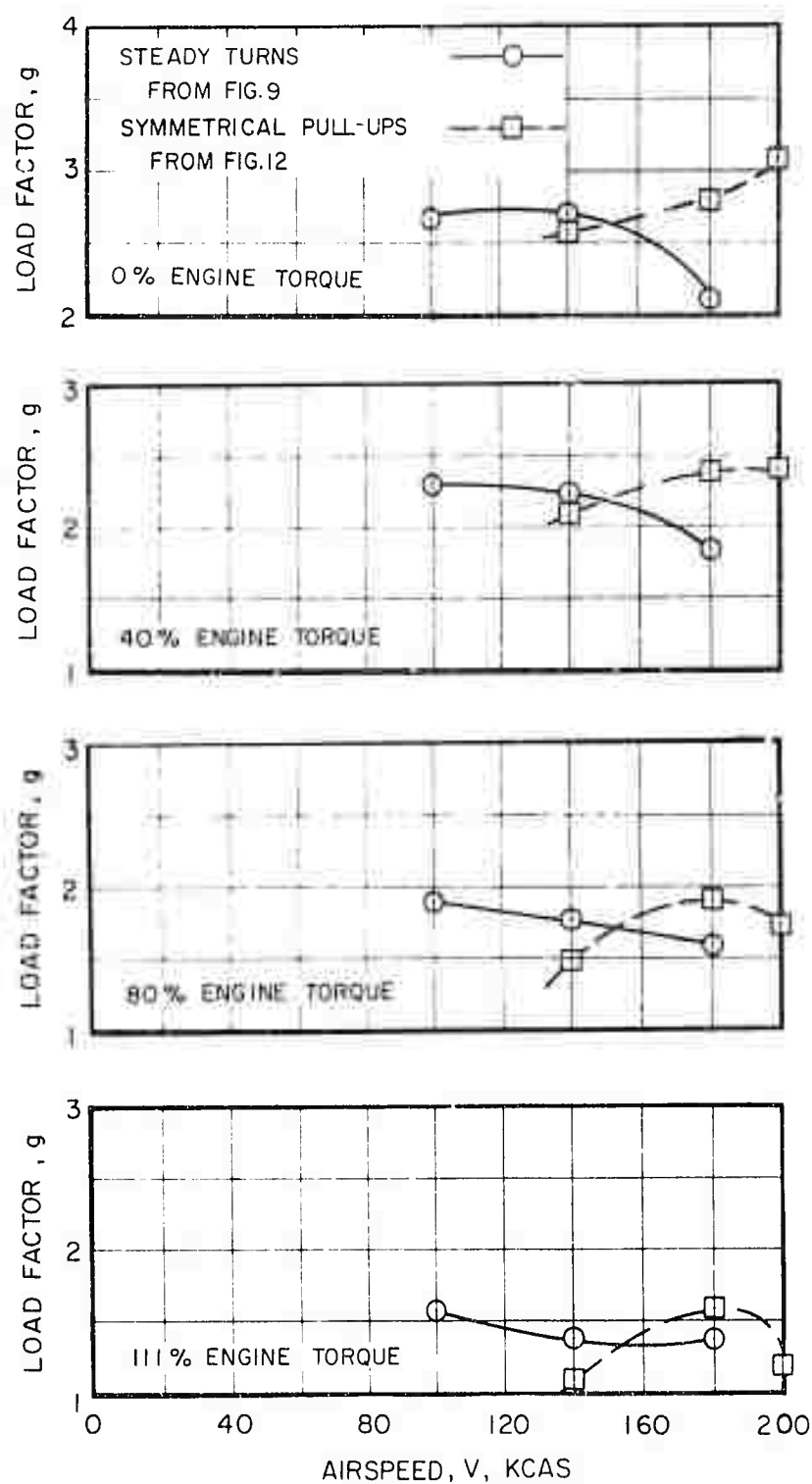


Figure 18. S-67 Load Factor vs Airspeed at 14,800 Lb, 276 C.G., Constant Engine Torque, Comparing Steady Turns and Pull-Ups.

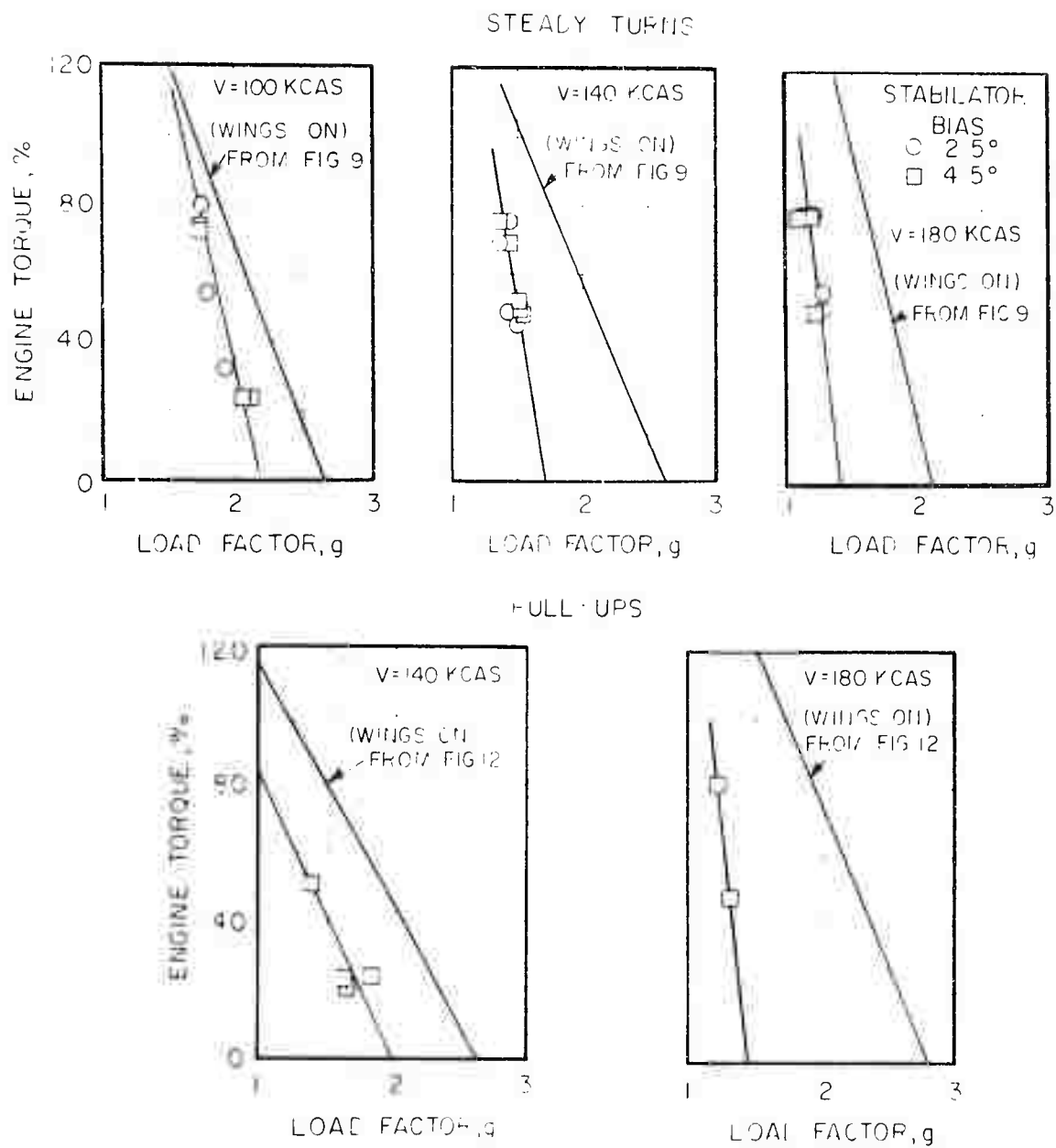


Figure 19. H-OF Primary Engine Torque vs Load Factor at 14,000 lb., 10 ft. H., Without Wings, for Various Speeds and Maneuvers.

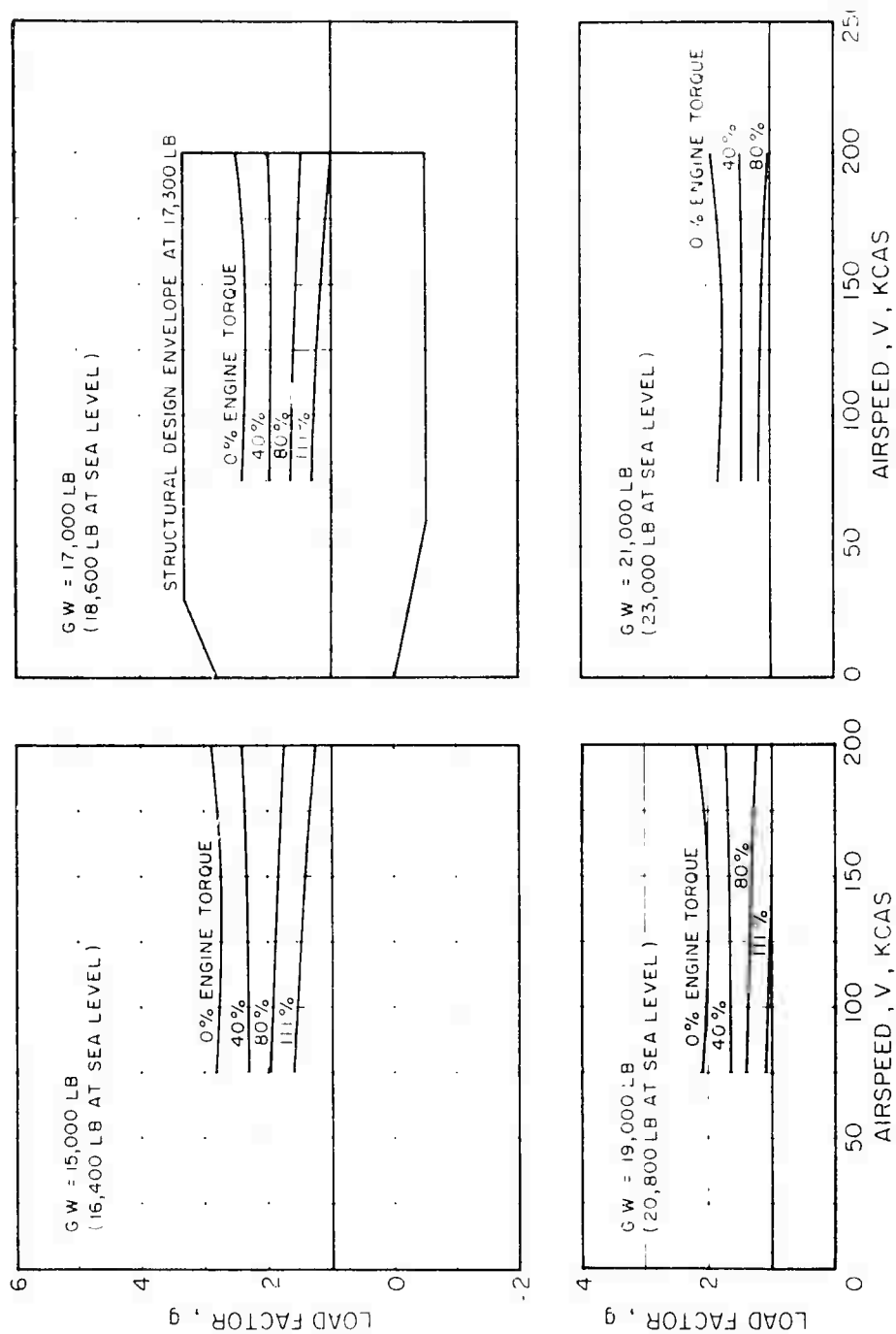


Figure 20. S-67 Load Factor Capability vs Airspeed at Constant Engine Torque and Gross Weights, Derived From Control-Load-Limited Flight Data at 3000 Ft Density Altitude.

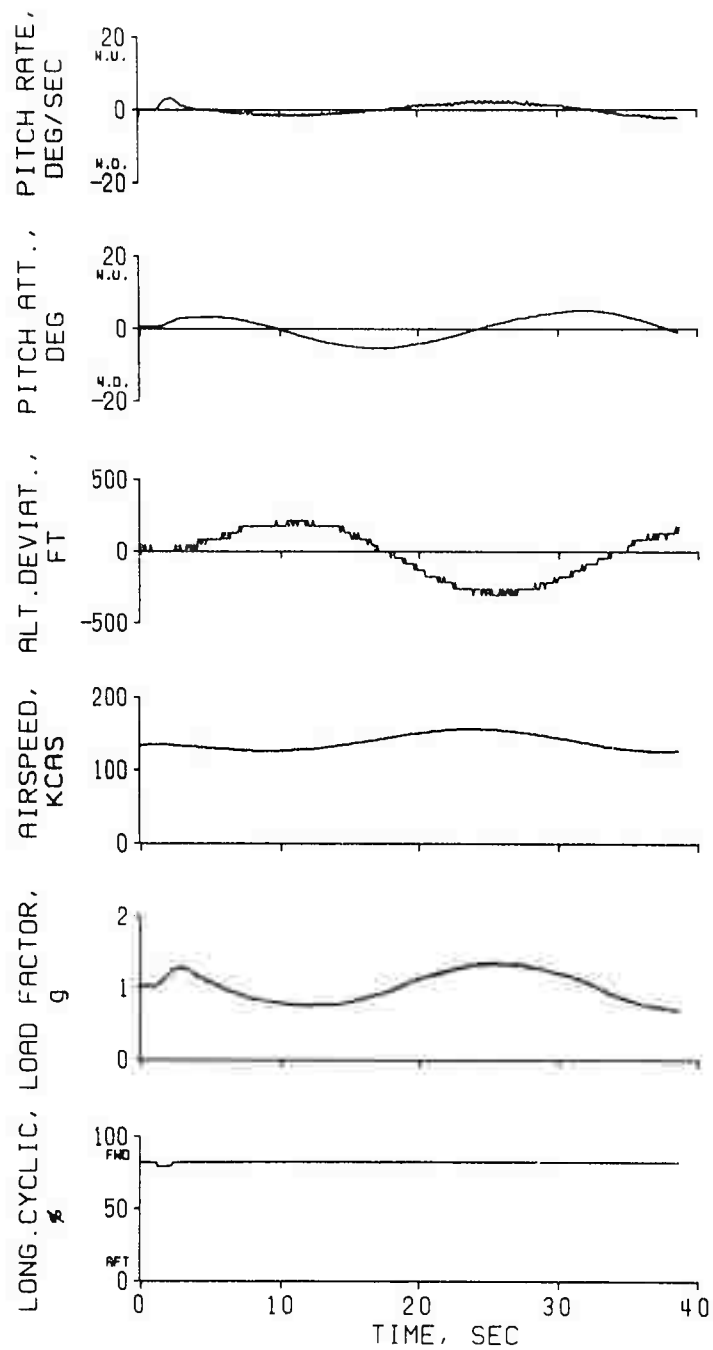


Figure 21. S-67 Longitudinal Stability, AFCS Off, at 14,800 Lb, 276 C.G., 140 KCAS, Following an Aft Cyclic Pulse.

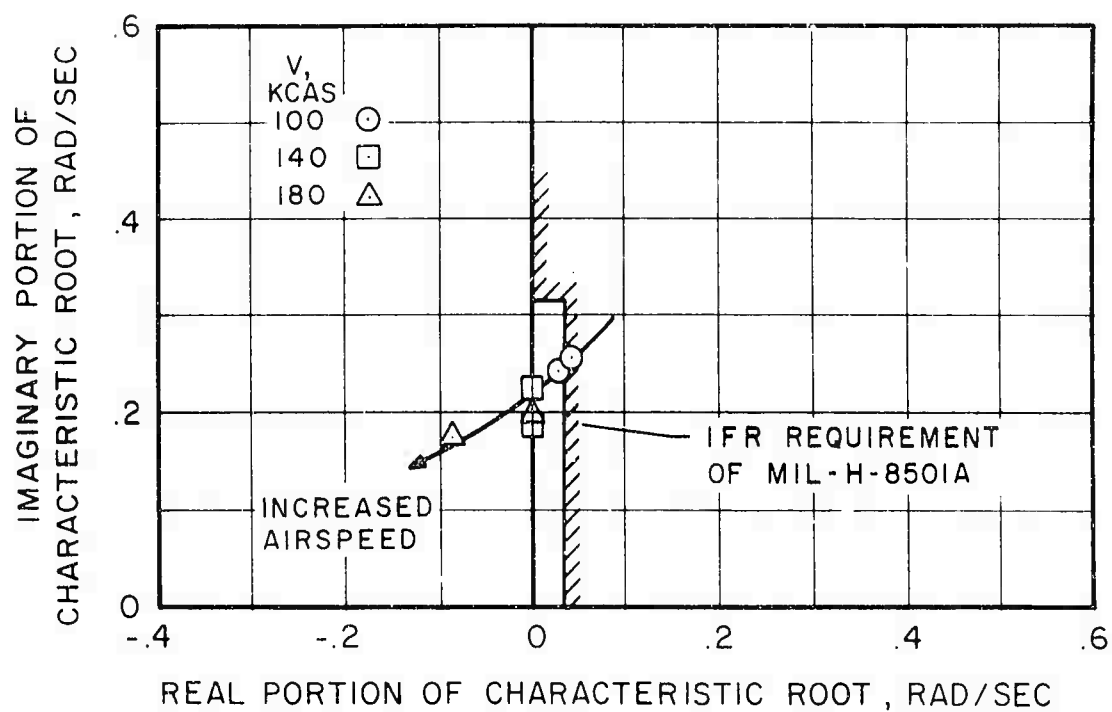


Figure 22. S-67 Summary of Longitudinal Characteristic Roots Derived From Time Histories of Aircraft Motion Following Control Pulses, AFCS Off, 14,800 Lb, 276 C.G.

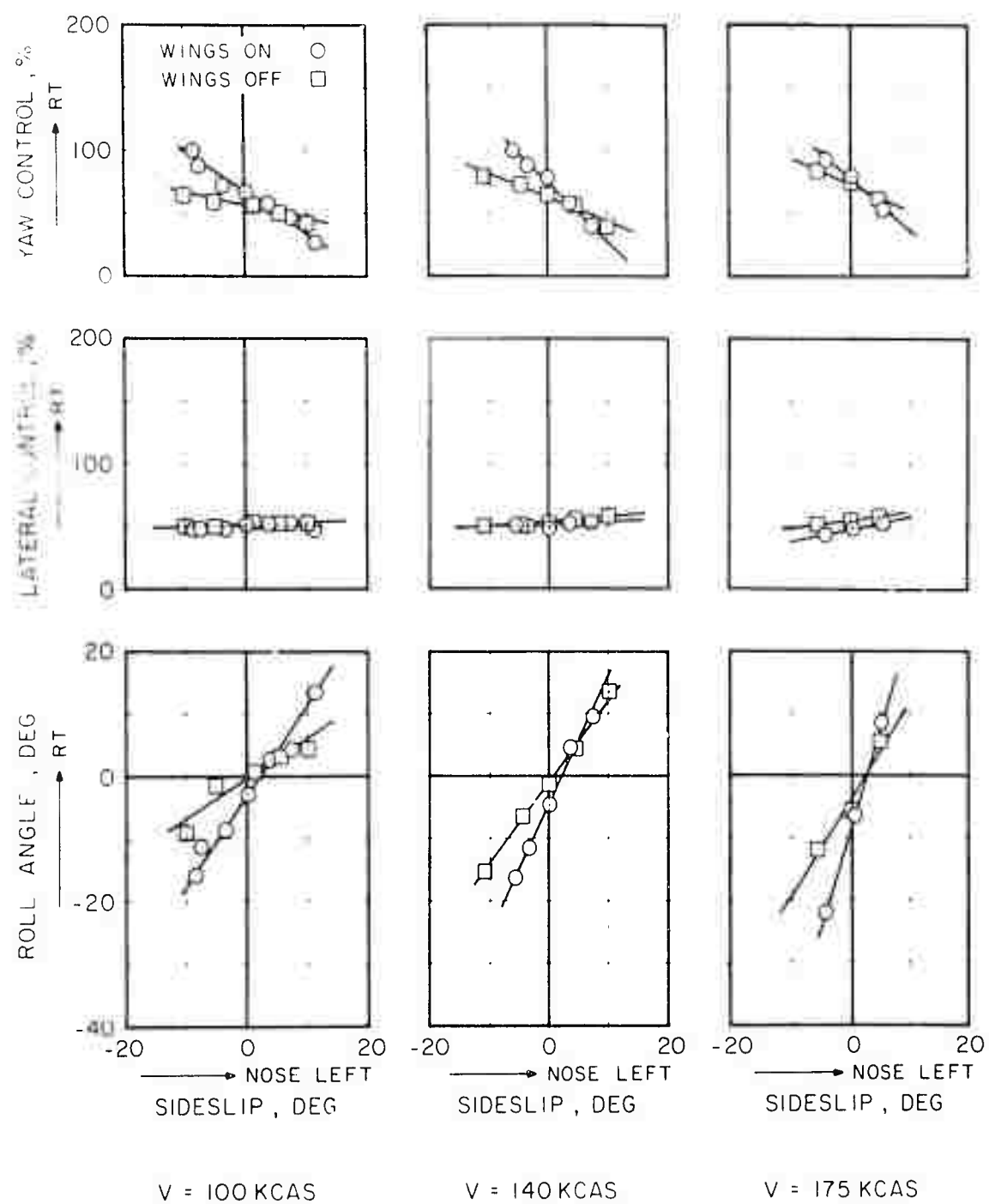


Figure 11. F-57 Lateral-Directional Trim Characteristics, Showing the Effect of Wings at 14,000 lb, 27° C.G.

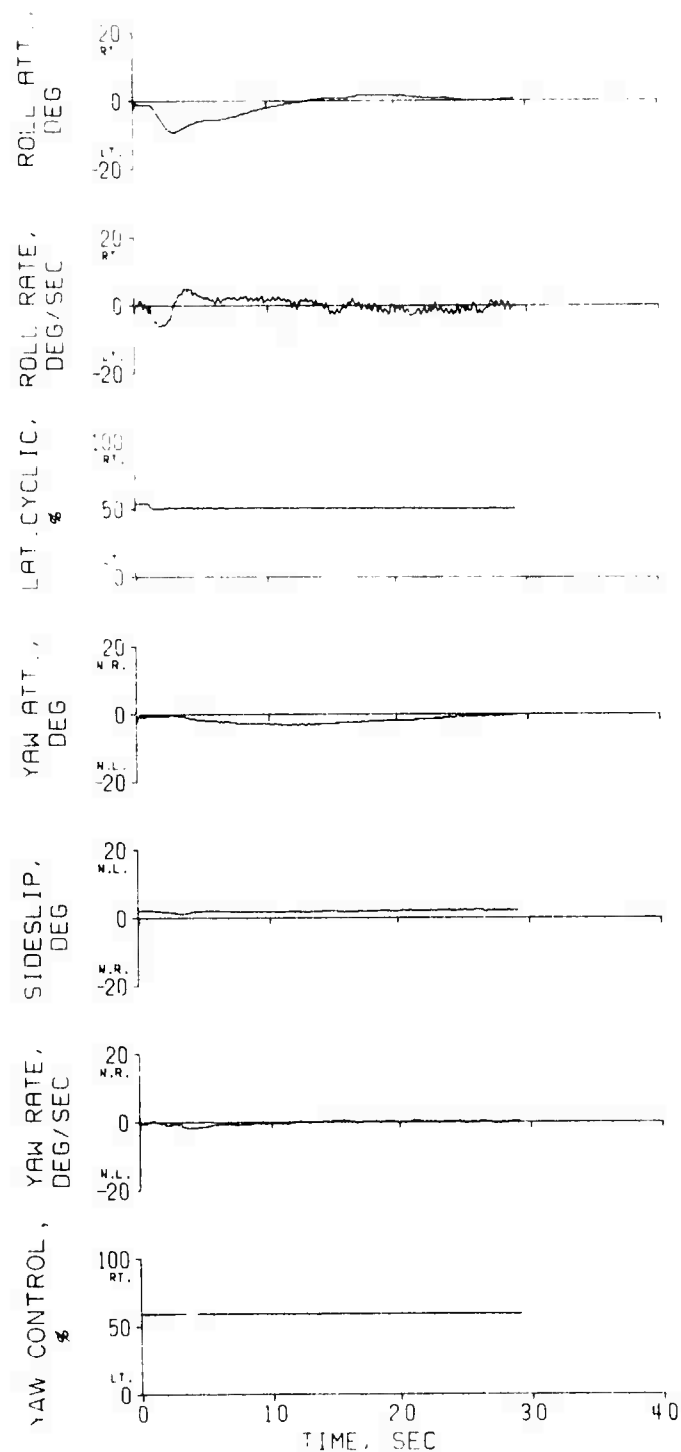


Figure 24. -07 Airplane-Directional Stability, AFCS Off,  $\alpha = 14.501$  deg, 270 C.G., 140 KCAS, Following a Left Lateral Cyclic Pulse.

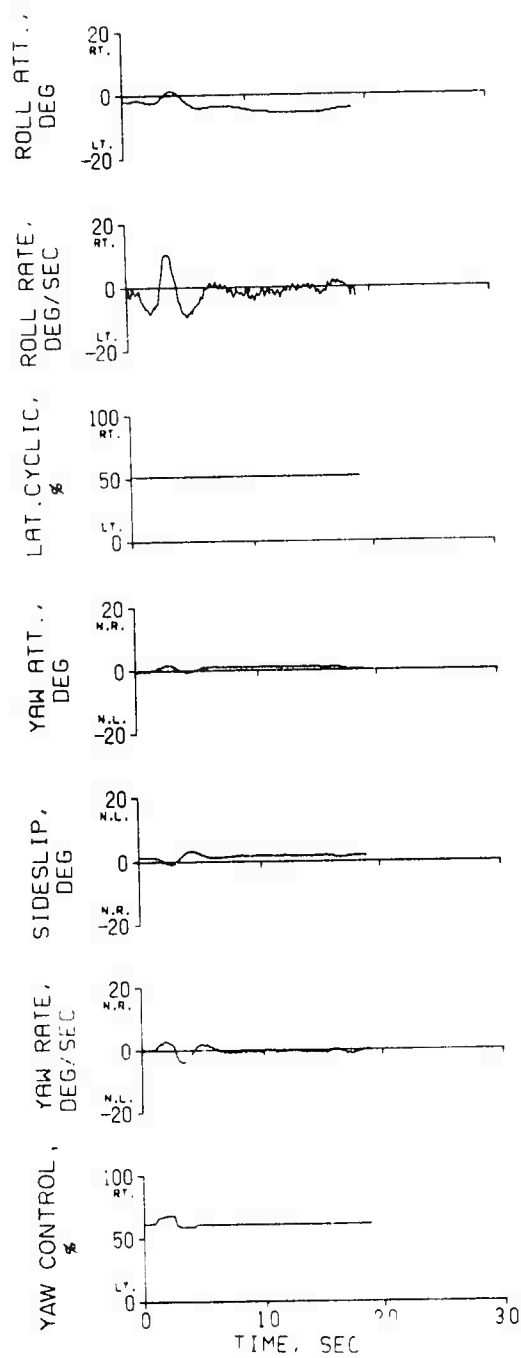


Figure 25. S-67 Lateral-Directional Stability, AFCS Off, at 14,800 Lb, 276 C.G., 140 KCAS, Following a Right Pedal Pulse.

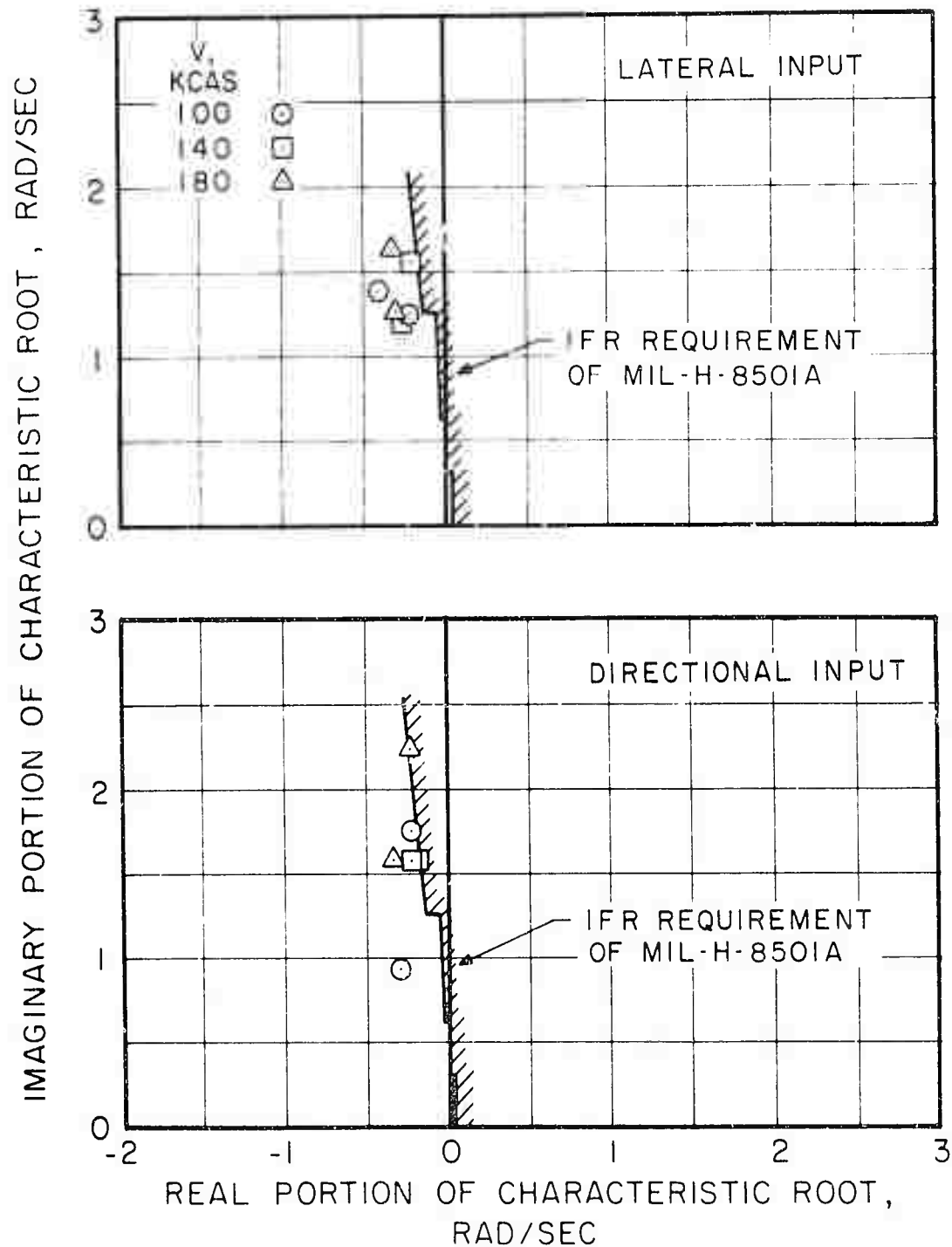


Figure 26. S-67 Summary of Lateral and Directional Characteristic Roots Derived From Time Histories of Aircraft Motion Following Control Pulses, AFCS Off, 14,800 Lb, 276 C.G.



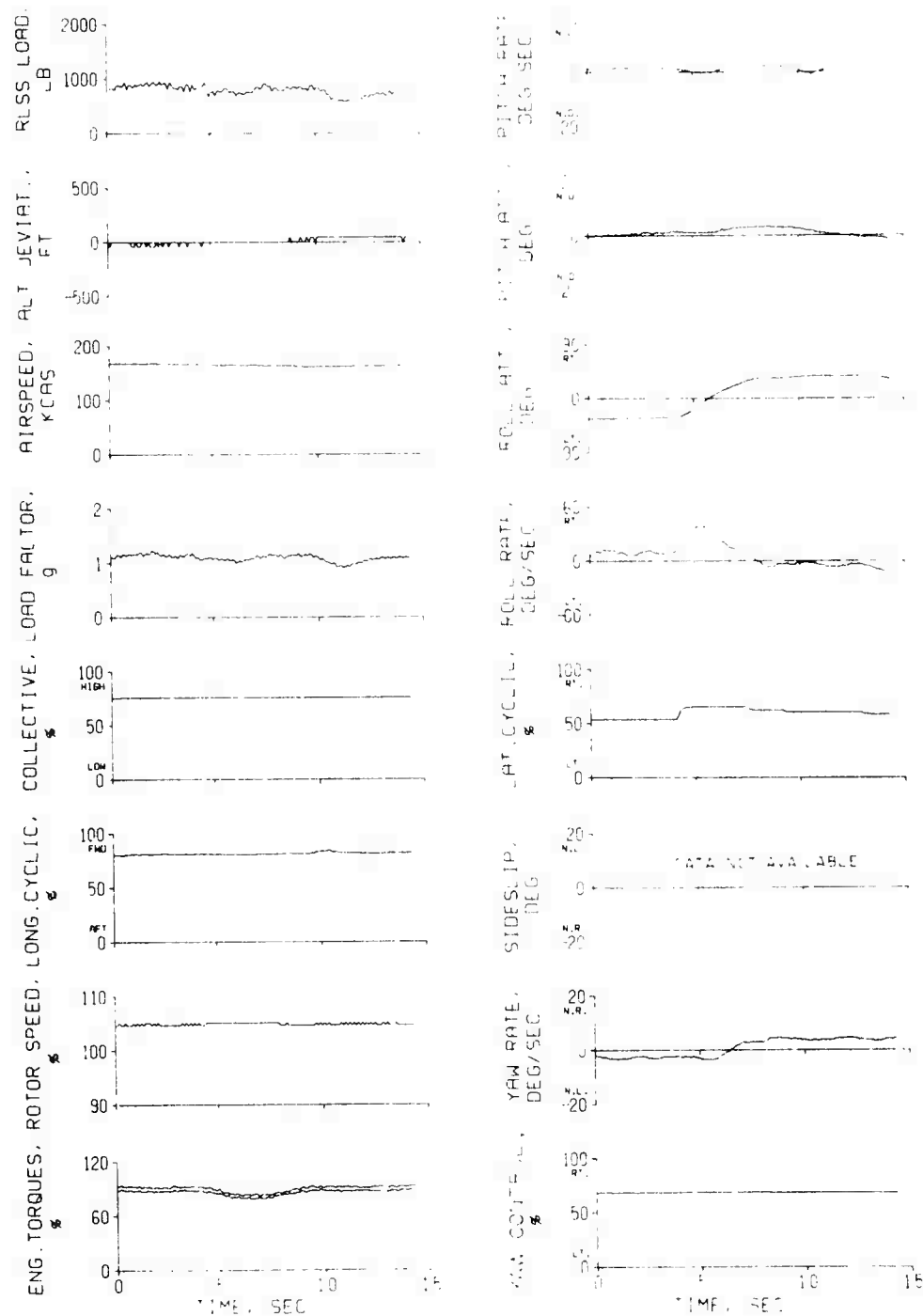


Figure 28. A-10 in level flight at 170 KCAS, Without Wings, 14,800 LB, 276 G, 4.5 Degrees Stabilizer Bias Angle.

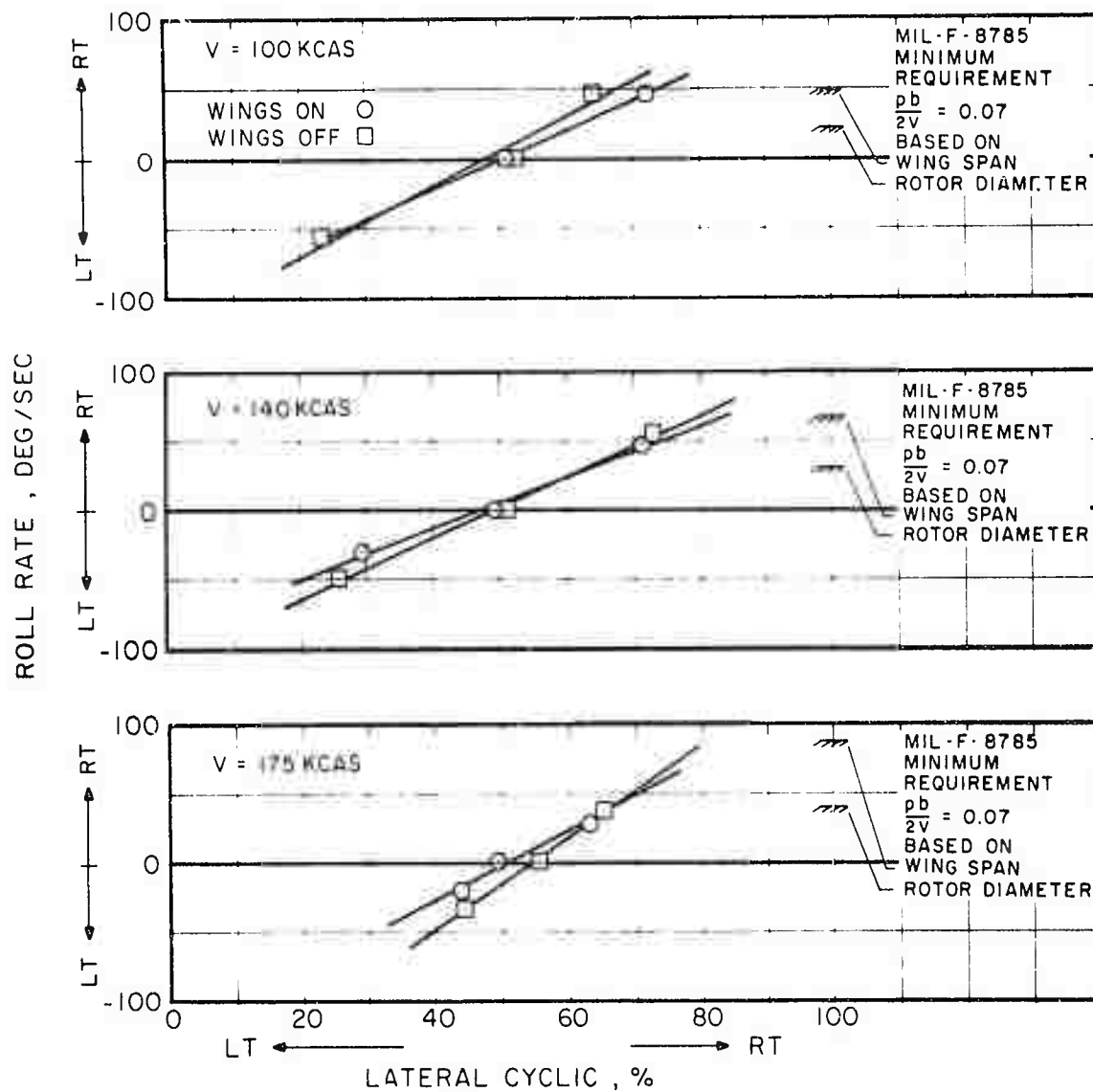


Figure 29. S-67 Roll Rate vs. Lateral Cyclic, Showing the Effect of Wings at 14,800 Lb, 276 C.G.

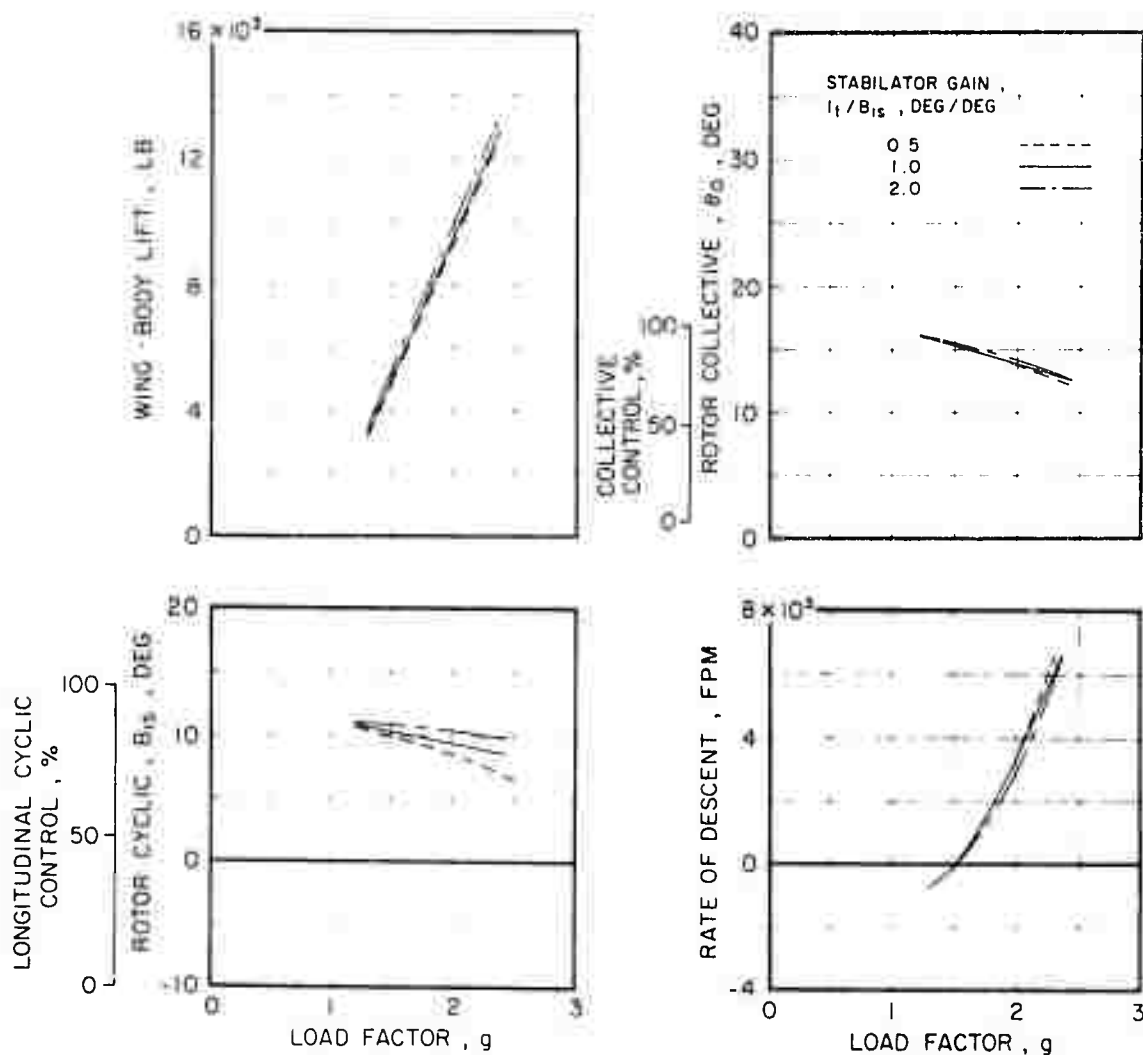


Figure 30. S-67 Simulator Data - Effect of Stick to Stabilator Gain in 180-KCAS, 2800-HP, Steady-State Descending Turns at 14,800 Lb, 276 C.G.

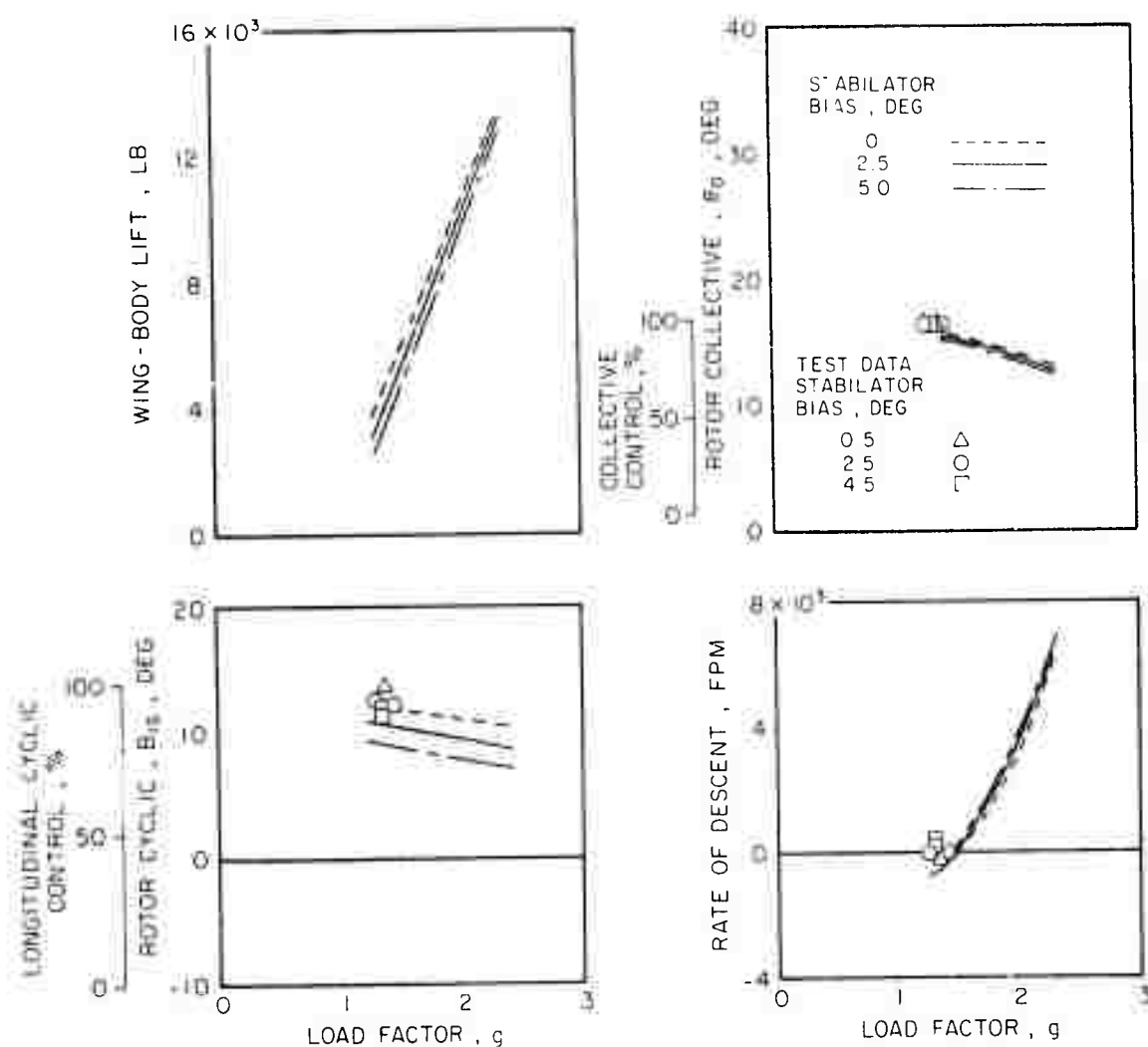


Figure 31. S-67 Simulator Data - Effect of Stabilator Bias Angle in 180-KCAS, 2000-HP, Steady-State Descending Turns at 14,800 Lb, 276 C.G.

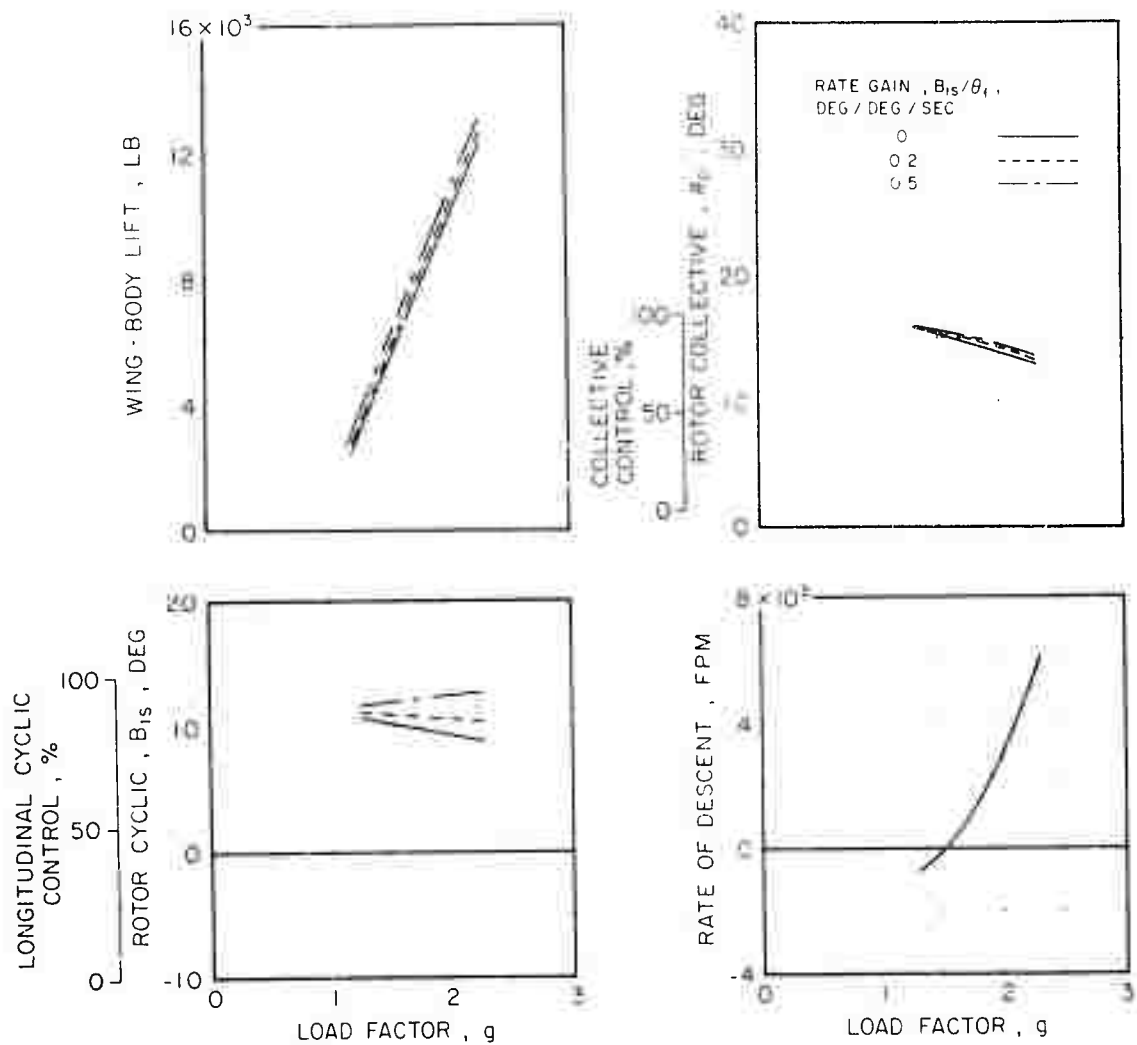


Figure 3. C-47 Simulator Data - effect of feedback to Rotor Cyclic on  $B_{15}$ , 1000-mph, Steady-State Descending Performance,  $\theta_1 = 1.1$ .

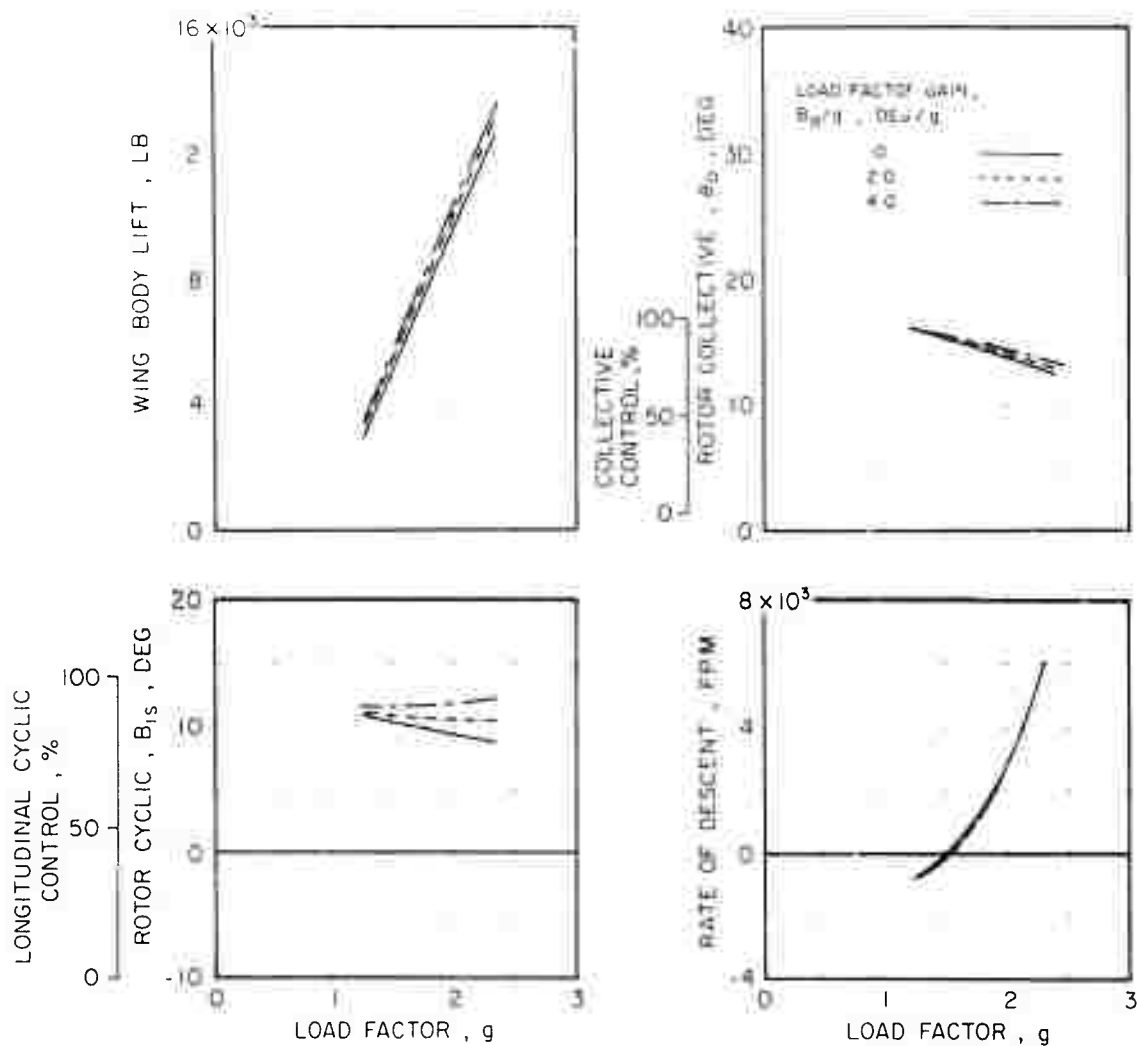


Figure 33. C-67 Simulator Data - Effect of Load Factor Feedback to Rotor Cyclic in 180-KCAS, 2800-HP, Steady-State Descending Turns at 14,800 Lb, 170 K.T.

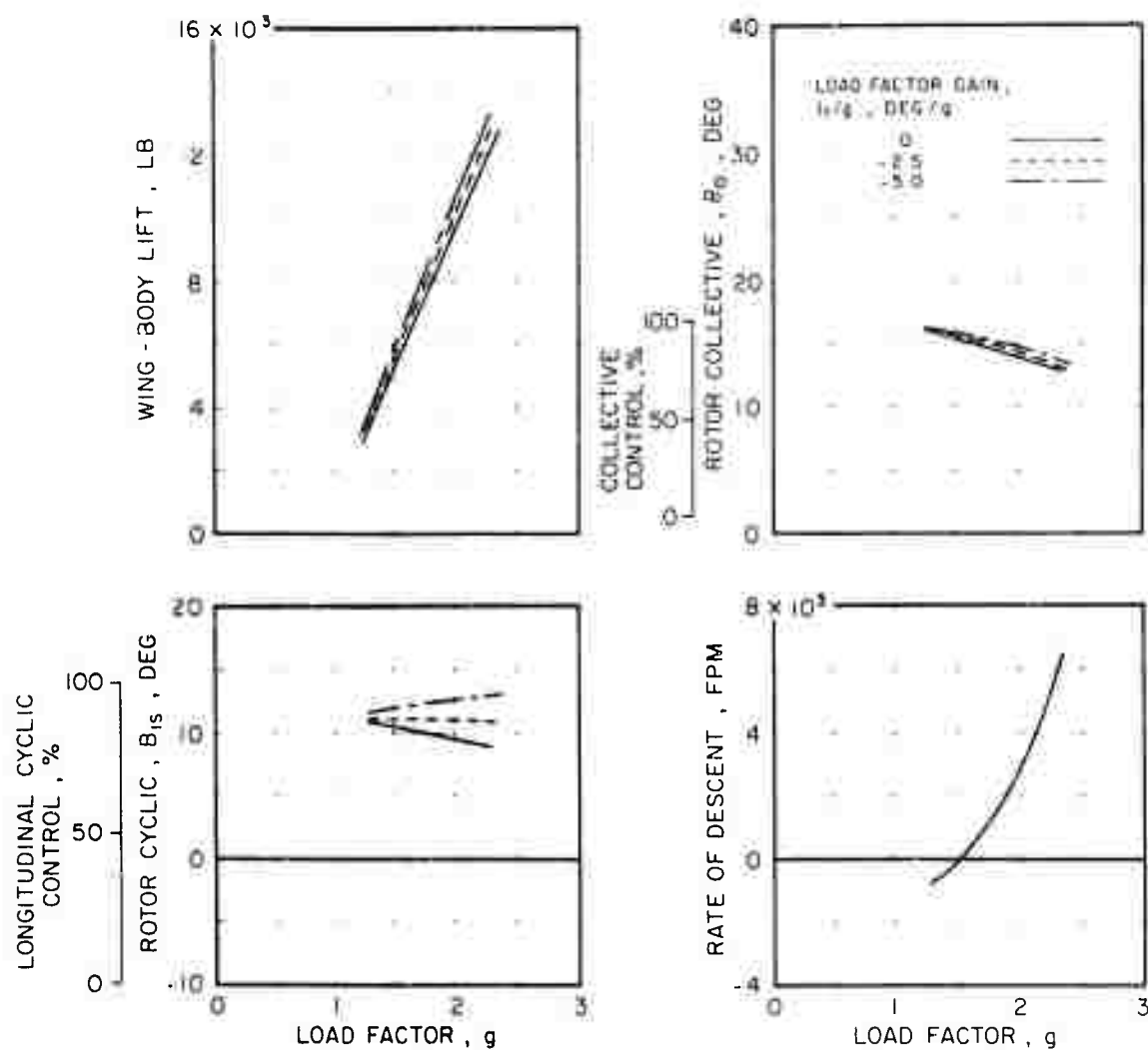


Figure 34. S-67 Simulator Data - Effect of Load Factor Coupling to Stabilator Incidence in 180-KCAS, 2800-HP, Steady-State Descending Turns at 14,800 Lb, 276 C.G.

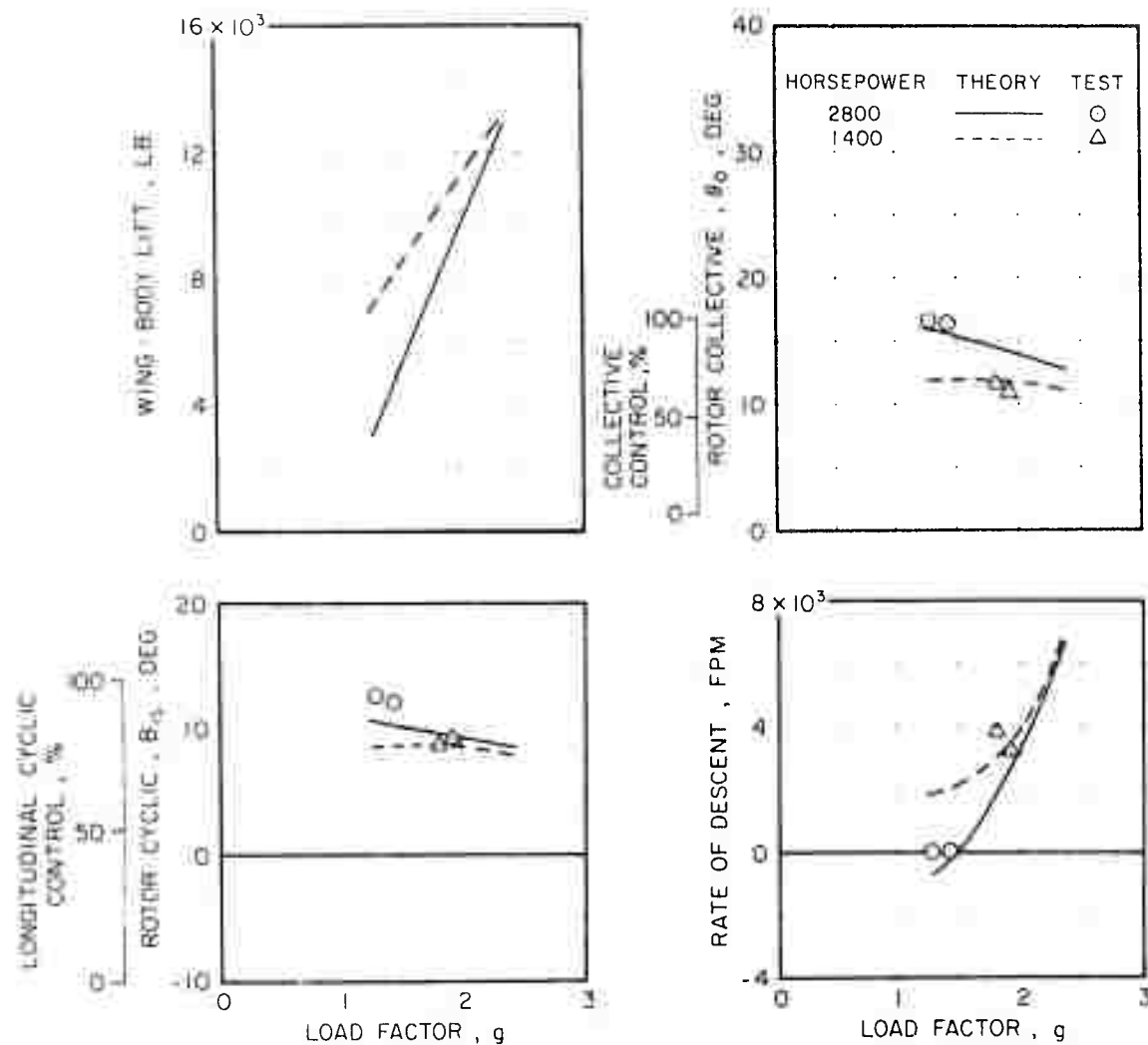


Figure 35. F-67 Simulator Data - Effect of Horsepower Variation in 180-KCAS, Steady-State Descending Turns at 14,800 Lb, 276 G.G.

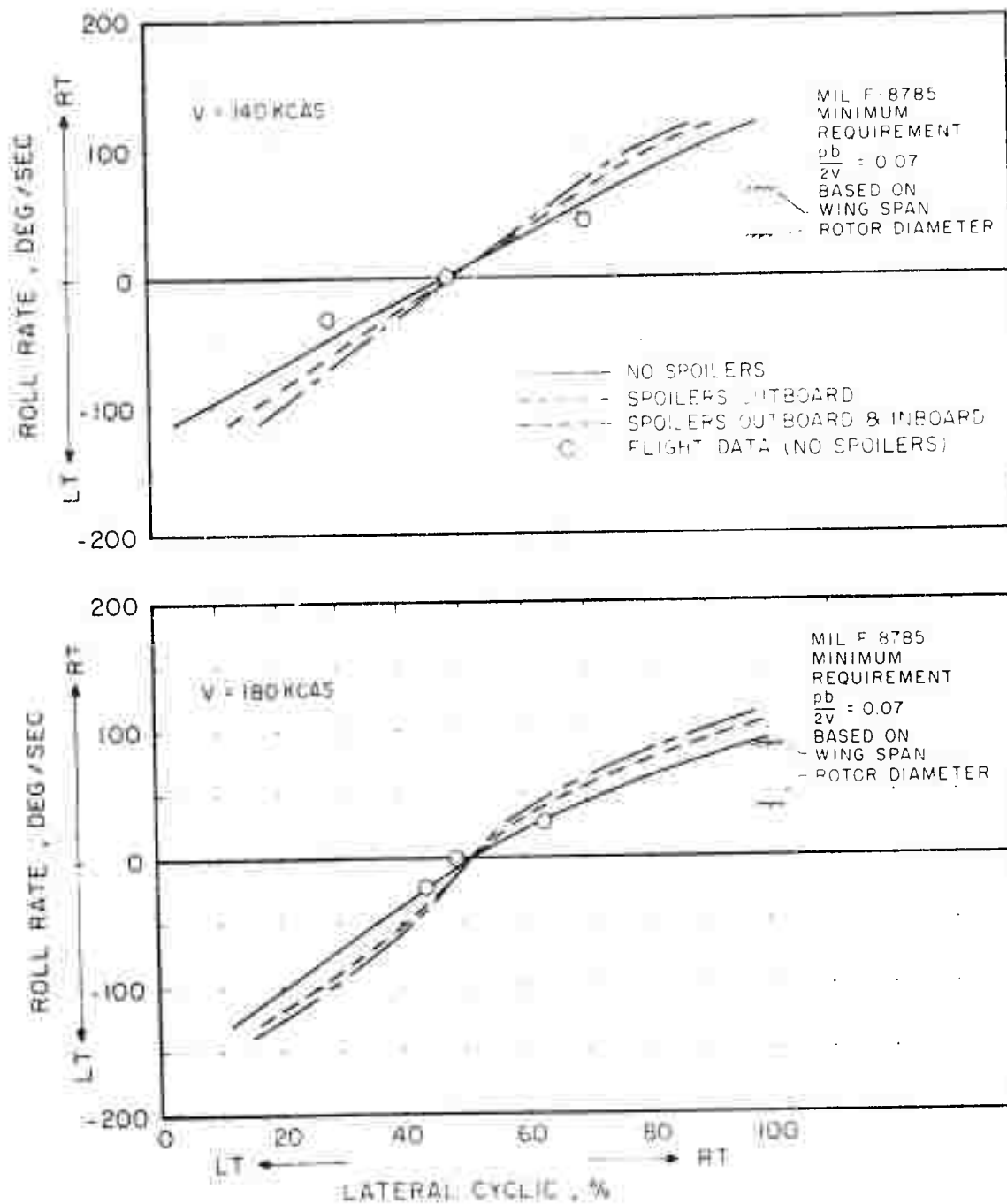


Figure 10. Roll Rate vs. Lateral Cyclic for MIL-F-8785 Minimum Requirement at V = 140 KCAS and V = 180 KCAS. The graphs show that the spoiler configurations generally meet or exceed the minimum requirement, with the 'SPOILERS OUTBOARD & INBOARD' configuration showing the highest roll rate.